Open Research Online

The Giant Lavas of Kalkarindji: rubbly phoehoe lava in an ancient continental flood basalt province

Journal Item

For guidance on citations see FAQs.

Version: Accepted Manuscript

oro.open.ac.uk

Palaeogeography, Palaeoclimatology, Palaeoecology

The Giant Lavas of Kalkarindji: rubbly pāhoehoe lava in an ancient continental flood basalt province

Peter E. Marshall*[a], Mike Widdowson[a†], David T. Murphy[b]

[a]Volcano Dynamics Group, Environment, Earth & Ecosystems, The Open University, Walton Hall, Milton Keynes, MK7 6AA, UK.

[b]Earth, Environment and Biological Sciences, Gardens Point Campus, Queensland University of Technology, Brisbane, QLD 4000, Australia.

†Now at: Department of Geography, Environment and Earth Sciences, University of Hull, Hull, HU6 7RX, UK.

*Corresponding author:

Mr Peter Marshall

email: peter.marshall@open.ac.uk

Abstract

The Kalkarindji continental flood basalt province of northern Australia erupted in the mid Cambrian (c. 511 - 505 Ma). It now consists of scattered basaltic lava fields, the most extensive being the Antrim Plateau Volcanics (APV) - a semi-continuous outcrop (c. 50,000 km^2) reaching a maximum thickness of 1.1 km. Cropping out predominately in the SW of the APV, close to the top of the basalt succession, lies the Blackfella Rockhole Member (BRM). Originally described as 'basaltic agglomerate' the BRM has, in recent years, been assumed to be explosive tephra of phreatomagmatic origin, thus providing a potent vehicle for volatile release to the upper atmosphere. Our detailed field investigations reveal that this basaltic agglomerate is, in reality, giant rubble collections (15 - 20 m thick) forming the upper crusts of rubbly pāhoehoe lava units 25 - 40 m thick; covering 18,000 - 72,000 km^2 and an estimated volume of 1,500 - 19,200 km^3. These flows, rheologically but not chemically, distinct from the majority of Kalkarindji lavas, indicate a fundamental change in eruption dynamics. A low volatile content, induced high amounts of pre-eruptive degassing causing super-cooling and an increase in crystal nucleation and viscosity. A more viscous lava and a consistently faster rate of effusion (analogous to that of Laki, Iceland) created the flow dynamics necessary to disturb the lava crust to the extent seen in the BRM. Volatile release is estimated at 1.65×10^4 - 2.11×10^5 Tg total CO_2 at a rate of 867 Tg a^{-1} and 9.07×10^3 - 1.16×10^5 Tg SO_2 at 476.50 Tg a^{-1}. These masses accounted for 0.5% of Cambrian atmospheric conditions whilst limiting factors reduced the effect of volatile delivery to the atmosphere, thus any potential global impact caused by these flows alone was minimal.

Keywords

1. Introduction

Continental flood basalt provinces (CFBPs) are huge eruptive events which have occurred not only in the Phanerozoic, but throughout Earth's history (Ernst et al., 2008, 2013; Bryan et al., 2010; Pirajno and Hoatson, 2012). The oldest Phanerozoic CFBP, Kalkarindji, covers a large tract of northern Australia. It was erupted onto the North Australian Craton during the mid-Cambrian period between 511 - 505 ± 2 Ma (Glass and Phillips, 2006; Evins et al., 2009; Jourdan et al., 2014), which formed part of Gondwana (Foden et al., 2006; Torsvik and Cocks, 2009; Cocks and Torsvik, 2013). The composition and morphology of CFBP lavas are known to vary significantly within a province (Walker, 1971; Bondre et al., 2004; Single and Jerram, 2004; Bryan et al., 2010; Brown et al., 2011; Duraiswami et al., 2014), but the common CFBP lava emplacement mode is as extensive pāhoehoe flow fields emplaced by a process of endogenous inflation, as observed occurring on the flanks of modern day shield volcanoes such as in Hawai'i (Self et al., 1997, 1998; Thordarson and Self, 1998; Bondre et al., 2004; Single and Jerram, 2004; Jerram and Widdowson, 2005; Waichel et al., 2006; Vye-Brown et al., 2013). Whilst this emplacement model is characteristic of the majority of the Kalkarindji basalt succession (Sweet et al., 1971; Bultitude, 1976; Mory and Beere, 1985), debate remains regarding the nature of the Blackfella Rockhole Member (BRM), because the appearance of these units differs significantly from those commonly observed in CFBP successions (Sweet et al., 1974; Mory and Beere, 1985; Jourdan et al., 2014). We address the emplacement of the BRM using extensive field observation, evaluate its eruption dynamics through petrography and geochemistry, and discuss whether, as proposed by Jourdan et al. (2014), it had the potential to cause global environmental change.

1.1. Geological background of the Kalkarindji CFBP

Today, the Kalkarindji CFBP consists of five individual sub-provinces which extend semi-continuously from the East Kimberley of Western Australia (WA), across Northern Territory (NT) to the Gulf Savannah of NW Queensland (Glass, 2002), another indicator of extent is a geochemically correlated dyke in the West

Kimberley of WA (Hanley and Wingate, 2000) (Fig. 1). Together these outcrops cover an estimated 55,000 km^2 (Bultitude, 1972, 1976; Cutovinos et al., 2002) and although controversial, if originally connected as a continuous expanse of lava fields, would have had an estimated areal extent of ~400,000 km^2 (Veevers, 2001), and a volume of ~1.5 x 10^5 km^3 (Glass and Phillips, 2006), thus making it comparable in size and volume to the well preserved Columbia River Basalt Province, USA (Coffin and Eldholm, 1994; Bryan et al., 2010). The Table Hill Volcanics (THV) of Western Australia, some 1000 km south of the APV, are also now considered part of the Kalkarindji province through geochemical, geochronological and stratigraphic correlation (Grey et al., 2005; Glass and Phillips, 2006; Evins et al., 2009) (Fig. 1). However, the lack of current outcrop, coupled with difficulties of inter-basin correlation between the THV and the Kalkarindji CFBP occurrences mitigates against the idea that there was once 'blanket coverage' of lava flows linking these two provinces.
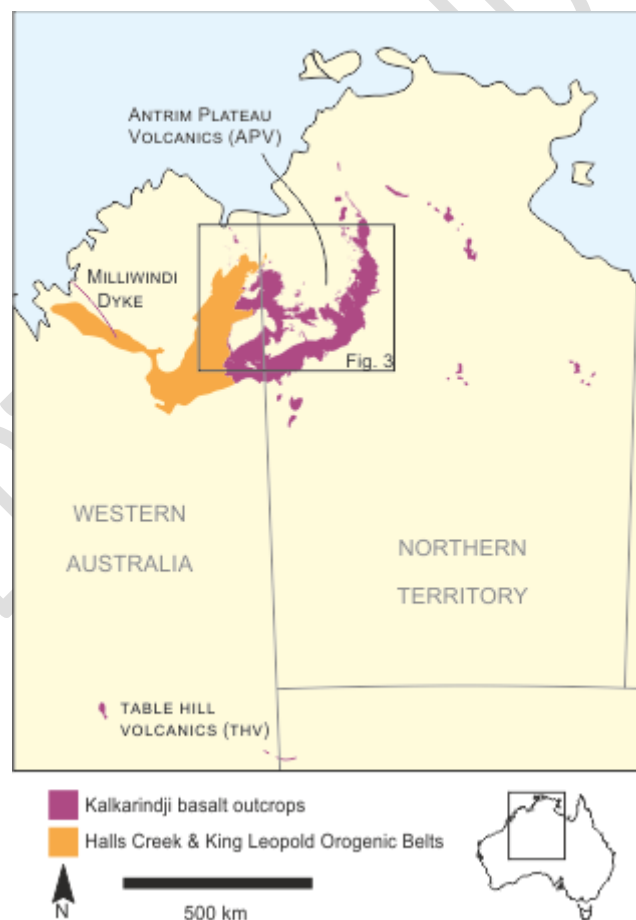

Figure 1: Schematic map of the modern day outcrop patterns of the constituent sub-provinces forming the Kalkarindji CFBP

The most extensive sub-province of Kalkarindji, the Antrim Plateau Volcanics (APV), crops out over a semi-continuous area of c. 50,000 km^2 in the Victoria River and East Kimberley Regions of NT and WA, with a maximum lava pile thickness of 1.1 km (Mory and Beere, 1988; Cutovinos et al., 2002). The APV succession unconformably overlies a series of Proterozoic sedimentary basins, the oldest and largest of which is the Birrindudu basin (1735 Ma - 1610 Ma), all of which contain a variety of quartz to arkosic sandstones (Sweet et al., 1974; Cutovinos et al., 2002). The basalts are in turn, disconformably overlain by stromatolitic limestones of Late Cambrian age deposited in several basins around the province. The Halls Creek Orogen is a long-lived belt of deformation (i.e. multiple reactivation episodes), which marks the western edge of the APV; this is a complex series of faults and thrusts involving units ranging from the Palaeoproterozoic through to Devonian and fragments of Kalkarindji basalt.

The majority of the APV basalt succession consists predominantly of inflated sheets of pāhoehoe lava; these remain largely undifferentiated stratigraphically, in part due to the poor exposure around the province and to their monotonous textural and internal similarities. Intercalated in this thick, undifferentiated lava stack, four members are identifiable within the APV sub-province: from lowest to highest, these are the Malley Springs Sandstone Member (3-5 m thick); the Mt. Close Chert Member (5 m thick); the Bingy Bingy Basalt Member, a highly-distinctive and readily recognisable flow field (c. 20 - 130 m thick) consisting of glomero-porphyritic plagioclase phenocrysts, commonly displaying well-developed columnar jointing; and, lying above this key marker horizon, the Blackfella Rockhole Member (c. 70 - 130 m thick), a laterally-extensive, thick volcanic breccia succession (Mory and Beere, 1988) (Fig. 2).

Figure 2: Schematic correlated stratigraphy of the Antrim Plateau Volcanics (Data synthesised from Traves, 1955; Dow et al., 1964; Sweet et al., 1974; Playford et al., 1975; Dow, 1980; Mory and Beere, 1988)

The currently mapped BRM crops out as a broadly 'horse-shoe' shaped pattern fringing the Ord basin in the west of the APV. Isolated mesa-cappings of rubble-topped flows also occur well beyond this extent, notably in the northern and easternmost peripheries of the APV. Exposed sections may be found on the slopes of laterally extensive mesas and consist of intercalated basaltic debris and aphyric basalt sheets first described by Sweet et al. (1974) as *"dominantly agglomerate, interstratified with basalt lava flows"*. This description was amended by Mory & Beere (1985) who opined that *"the agglomerate represents the upper part of single lava flows and that the fine-grained basalt and agglomerate should be included within one unit."* They further extended the mapped extent of the BRM, providing detail of its extent predominately confined to the SW of the APV (Sweet et al., 1974; Mory and Beere, 1985, 1988; Cutovinos et al., 2002). However, this study has discovered previously unrecorded outcrops occurring in the North and East of the APV, suggesting this member to have once been far more extensive than is currently mapped (Fig. 3).
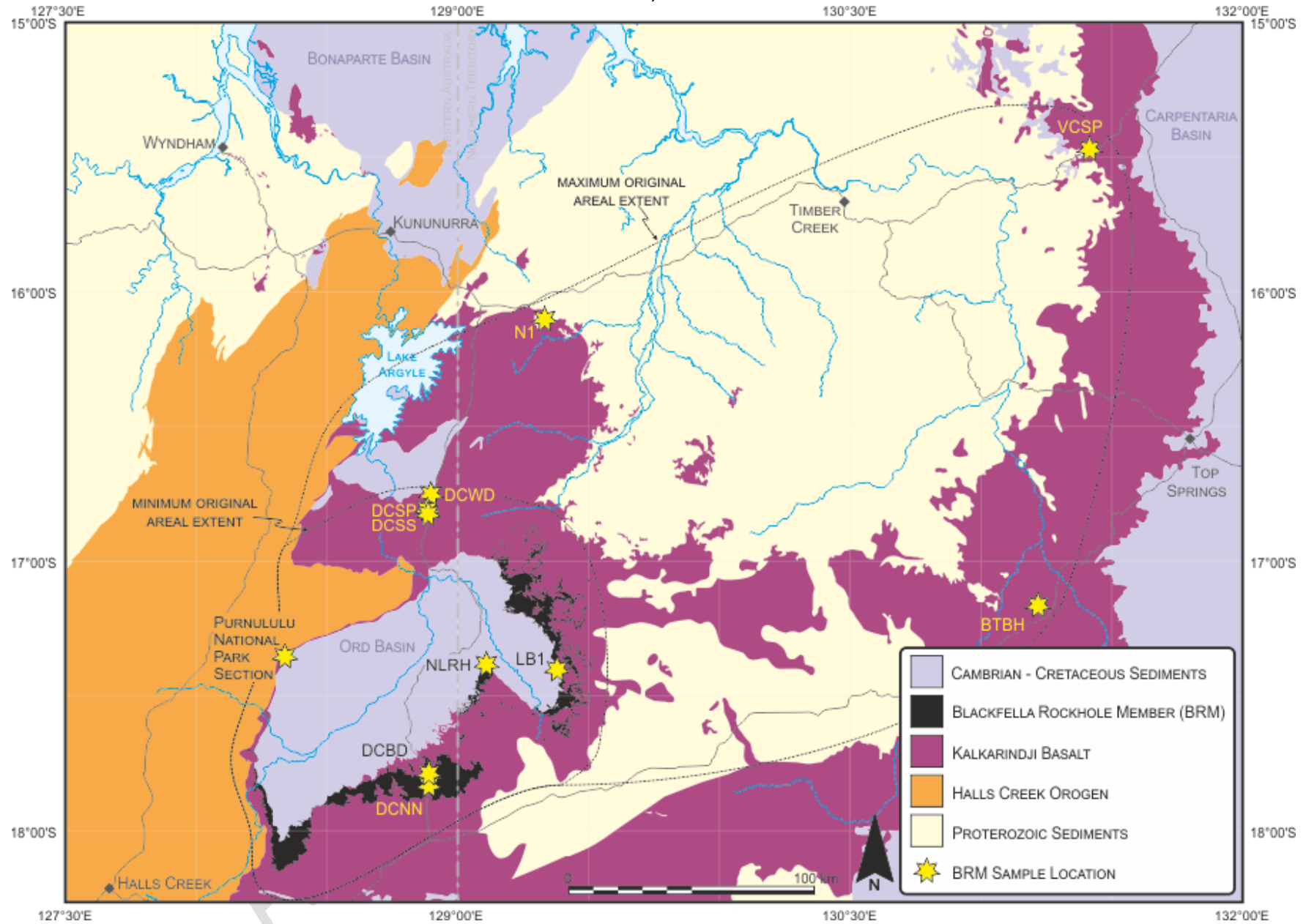
Figure 3: Outcrop map of the Antrim Plateau Volcanics in Western Australia and Northern Territory. The Blackfella Rockhole Member, highlighted in black, outcrops mainly in the SW of the province with occurrences noted to the north and east of the Ord basin.

An unintended result of the Sweet et al. (1974) description has been an unsuccessful search for eruptive vent locations within the province. This originates from the belief that the original description of 'basaltic agglomerate' was a genetic term, and thus indicative of an explosive, tephritic origin and composition; this has led to inevitable comparison with types of material associated with vent sites identified in other LIPs (Ross et al., 2005; Guilbaud et al., 2007; Brown et al., 2014). Further, inference of explosive volcanism has led to the idea of phreatomagmatism as a driver for BRM eruption and associated environmental change (Jourdan et al., 2014). Despite a number of detailed surveys by Northern Territory Geological Survey (NTGS), and during this study, vent locations within the province remain undetected. Instead, the current outcrop pattern of the BRM fringing the Ord Basin strongly indicates a source somewhere within the basin, now buried by the subsequent sedimentation of Cambrian and Devonian sediments. It remains to be determined whether this area was the only eruptive source of the APV. In order to understand the emplacement mechanics of the BRM, it is necessary to determine its nature, whether or not it represents repeated explosive events or, alternatively, autobrecciated rubbly lava flows erupted at the close of the APV (Kalkarindji) volcanic episode.

2. Field observations

Initially BRM outcrop was mapped using an easily identified brecciated flow unit which could be traced extensively using aerial photograph interpretation and selective ground reconnaissance (Sweet et al., 1974; Cutovinos et al., 2002). Detailed reconnaissance fieldwork and stratigraphic logging was conducted throughout the whole APV sub-province during three field seasons (2011 - 2013). Outcrop of BRM was found in several disparate locations, each with different characteristics, but we were able to correlate similarities between outcrops. Here we focus on detailed observations of the BRM at four specific localities, (i) the type locality at Blackfella Rockhole (NLRH), (ii) a tilted section in Purnululu National Park, (iii) locations to the south of the Ord basin (DCBD, DCNN) and (iv) north of the basin (DCSP, DCSS, DCWD). Other important outcrops were also investigated in the north-west (N1), and in the south-east of the APV (BTBH), whilst examination of borehole stratigraphy (LB1) on the Ord basin periphery has revealed the full thickness of a BRM unit (Table 1

& Fig. 3). Outcrop in the far north-east (VCSP) of the province is also noted displaying similar textures to BRM

outcrops (S. Planke, pers. comm.).

Table 1: Locations and descriptions of the key outcrops of BRM lava.

Locality	Coordinates (dd°mm'ss.s")	Elevation (m. a.s.l.)	No of flows	Description
NLRH	17°23'35.0"S 129°06'27.8"E	220	3-5	Type locality: Large river cut cliff sections exposing continuous section of giant rubbly pāhoehoe flows (70 m) from river bed to overlying limestone.
Purnululu National Park	17°21'53.1"S, 128°19'36.3"E	313	8-10	Tilted section in the Purnululu National Park exposing a full section from Precambrian basement through to overlying limestone with rubbly pāhoehoe flows stacked at the top of the basalt.
DCBD	17°48'27.5"S 128°53'15.8"E	377	2	Flow core at the roadside, a small stream cuts down into the valley where a larger river has cut a cliff through one full flow, down to the surface of flow-top beneath.
DCNN	17°51'00.4"S 128°53'30.3"E	432	2	Hummocky outcrops of rubble at roadside, larger hillocks away from the road form the core of the overlying flow. Sampled upper flow core.
DCSP	16°48'43.3"S 128°53'10.4"E	186	3	Lowermost flow core at the roadside sampled, hills above the road contain benches of horizontal rubbly lava flows.
DCSS	16°49'11.4"S 128°53'09.3"E	199	2	Large cliff of rubbly basalt at the roadside near entrance to Spring Creek Station. This is the flow top of the core found at DCSP, with a flow core above. Upper flow core sampled.
DCWD	16°45'31.3"S 128°54'09.9"E	198	3	On the southern arm of the Rosewood syncline, a series of flows are obvious in the hillside, marked by benches. Samples taken from road cuttings through lowermost flow core.
N1	16°06'05.5"S 129°19'43.8"E	229	1?	A large mesa, capped by an 85 m flow of massive basalt topped with rubble, directly overlying Proterozoic sandstone basement (Clark, 2014).
BTBH	17°10'39.1"S 131°12'14.6"E	271	1	Outcrop sits atop an isolated mesa, Biri Hill, 80 m above surrounding basalt plain.
LB1	17°25'00.0"S 129°22'37.7"E	298	2	Borehole drilled by BMR (Bultitude, 1971). Chips stored at Geoscience Australia archives, Canberra. Analysis of chips in 5 ft (1.5 m) intervals.
VCSP	15°28'S 131°23'E	208	1?	Outcrop of rubbly pāhoehoe looking basalt on northern edge of Victoria Highway (HWY 1). Information supplied by S Planke (pers. comm.).

2.1. Blackfella Rockhole (NLRH)

Sweet et al. (1974) defined a type section for the BRM at Blackfella Rockhole; this locale, where an unnamed

tributary of the Headley Creek cuts across the monocline associated with the NW-SE trending Negri Fault,

consists of a series of steep cliffs cut by the river, exposing a near continuous thickness of 70 m from the base

of the riverbed to the uppermost flow. South of the fault and associated monocline, the stratigraphy is near

flat lying and thus consistent with the majority of the APV succession (i.e. a dip of <1° to the south). Here, three individual volcanic units are present stacked one upon another and each consisting of a massive basalt - basaltic breccia transition; closer inspection reveals no evidence of intervening weathering or interbeds. In detail, each unit consists of an aphyric basalt core, generally devoid of internal structure, vesicles or phenocrysts. The bases of these massive flow cores have abrupt contacts with the brecciated rubble surface of the underlying unit via thin chill-zones (Fig. 4a). At the core - rubble-top transition distinct vesicular 'pods' occur dispersed within the top layers of aphyric basalt. These pods, roughly 15 – 20 cm in diameter, are fine-grained vesicular basalt masses containing abundant, small (mm – cm scale) mainly spherical vesicles, entirely surrounded by a fine-grained rind. These rinds are gradational, rather than sharp, blurring the edges of vesicles into the basalt matrix, indicating they have undergone partial assimilation or 'digestion' by the surrounding basalt (Fig. 4b). Mixed in at the same horizon are small (10 – 30 cm) clasts of variously coloured (different degrees of oxidation), aphyric basalt. In some instances these pods and clasts occur together with large, flattened gas blisters (10 – 25 cm) typically infilled by chalcedonic quartz; these appear to represent coalescence of a degassing vesicle load beneath a solidifying lava carapace (Fig. 4c). In the uppermost unit, the transition zone is well defined by a 2 m layer of basalt displaying horizontally 'platy' fabrics, sitting directly between the core and the thick rubble above (Fig. 4d). Importantly, in all three units there is an internal transition from undifferentiated, degassed flow core, through increasing sizes and proportion of partially digested clast material, up into a rubbly carapace layer: the agglomerate that sits atop the uppermost flow consists of a continuous >15 m thickness of rubble which forms the characteristic steep cliffs along the river valley.

In detail, the rubble capping all three units consists of randomly orientated, angular blocks (30 – 100 cm) containing remnants of lava crust textures such as fragments of ropey and slabbly pāhoehoe (Guilbaud et al., 2005; Sheth et al., 2015), squeeze-out spindles, sheared and distorted vesicles and minor injections of aphyric basalt. This rubble mass grades upwards from small clasts (~10 cm) supported in a degassed basalt matrix, into a clast-supported rubble of larger blocks (>50cm) at the top. Within this upper rubbly part several lava protrusions, (Fig. 4e) have developed where aphanitic basalt has punched its way upwards from the core,

through the rubble, to emerge as tumuli break-outs atop the overlying rubble pile (Duraiswami et al., 2001). Within the uppermost sections of the rubble of each unit, minor magma 'squeeze-outs' and internal injections from the core can be readily identified indicating that core and rubble are coeval components of the unit. Accordingly, we interpret these type locality BRM units as rubbly-topped lava flows, as originally described by Mory and Beere (1985), with the rubble layers being an autobrecciation product generated by rapid inflation and propagation of individual units within the BRM lava field.
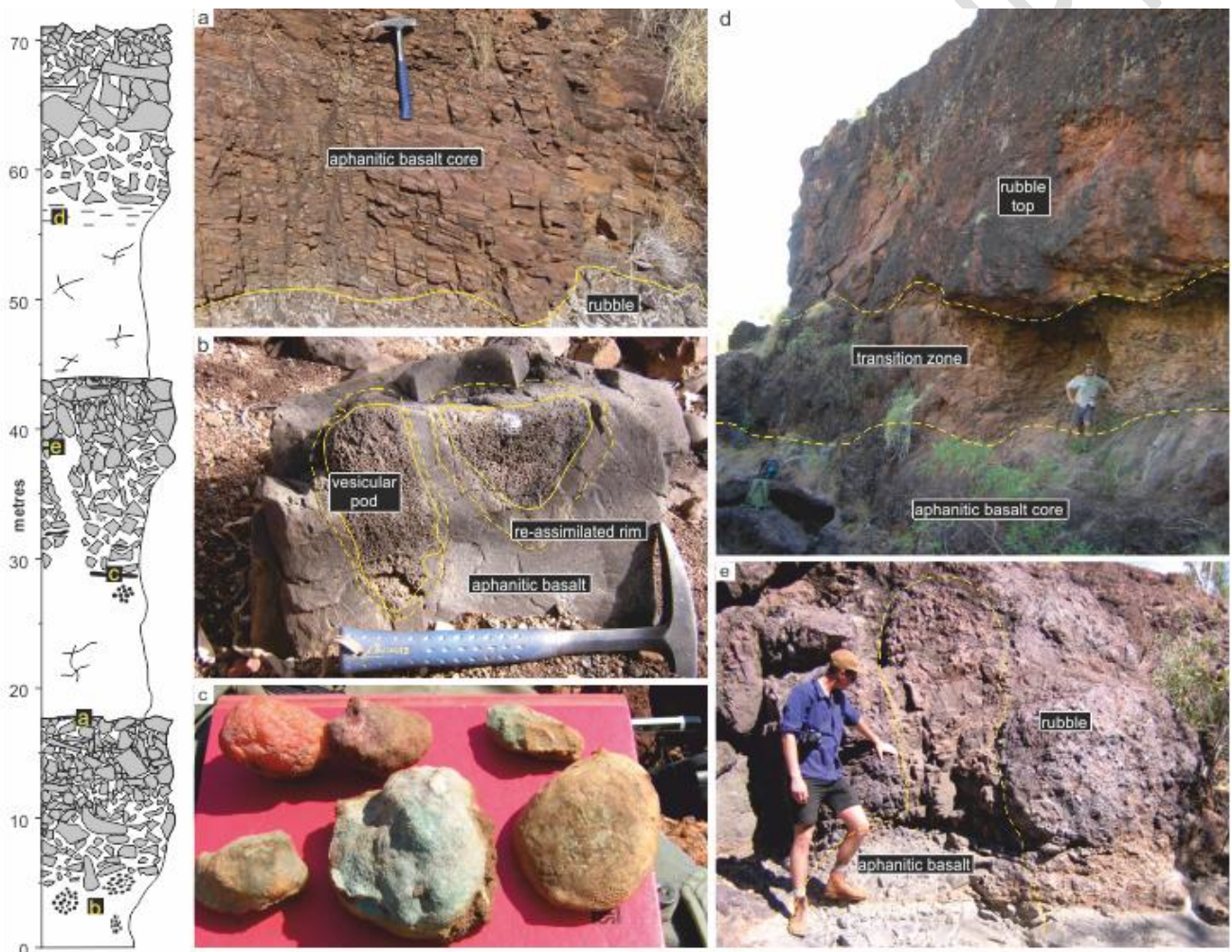
Figure 4: Summary log and field photographs from the type locality Blackfella Rockhole. a) Abrupt contact between the aphanitic flow core and the rubble top of the flow below. b) Vesicular pods containing mainly spherical vesicles, being partially assimilated into the flow core. c) Large flattened gas blisters (10 - 25 cm) often infilled by chalcedonic quartz. d) Platy fabrics of the transition zone sititng directly beneath the large rubble top. e) Example of a lava protrusion injected into the overlying rubble pile.

2.2. Purnululu National Park

Purnululu National Park, a UNESCO world heritage site in the Kimberley region of Western Australia lies within the western Ord Basin and preserves a thick Palaeozoic succession including the APV and overlying Cambrian - Devonian sediment successions. These successions lie unconformably upon Late Proterozoic sandstone basement. In the west of the park, the succession dips at c. 10 -25° eastward providing access to c. 750 m thickness through the mid and upper APV succession (comprising > 15 flows; Glass, 2002). A 1 km traverse E-W across the terrain (17°21'53.1"S, 128°19'36.3"E - 17°21'54.4"S, 128°19'26.9"E; Fig. 3) reveals the uppermost 150 m of this succession to be BRM consisting of 8 - 10 rubble-topped units occurring above a paler coloured basaltic unit, here interpreted as an outcrop of the Bingy-Bingy Basalt member. The BRM is capped by a prominent, semi-continuous ridge of overlying limestone.

The lateral extent of these Purnululu BRM flows of can be easily traced in the local topography, and on satellite imagery for several kms as a series of 10 – 25 m high, approximately north- south trending ridges. The resistant, steeper scarp slopes and summits are the massive fine-grained cores of each unit; the dip slopes corresponding to preferential stripping of the associated rubble tops. Each rubble-topped unit is c. 10 – 20 m thick and consists of broadly the same internal components as those identified at the type locality, summarised in the generalised section and field photos in figure 5.
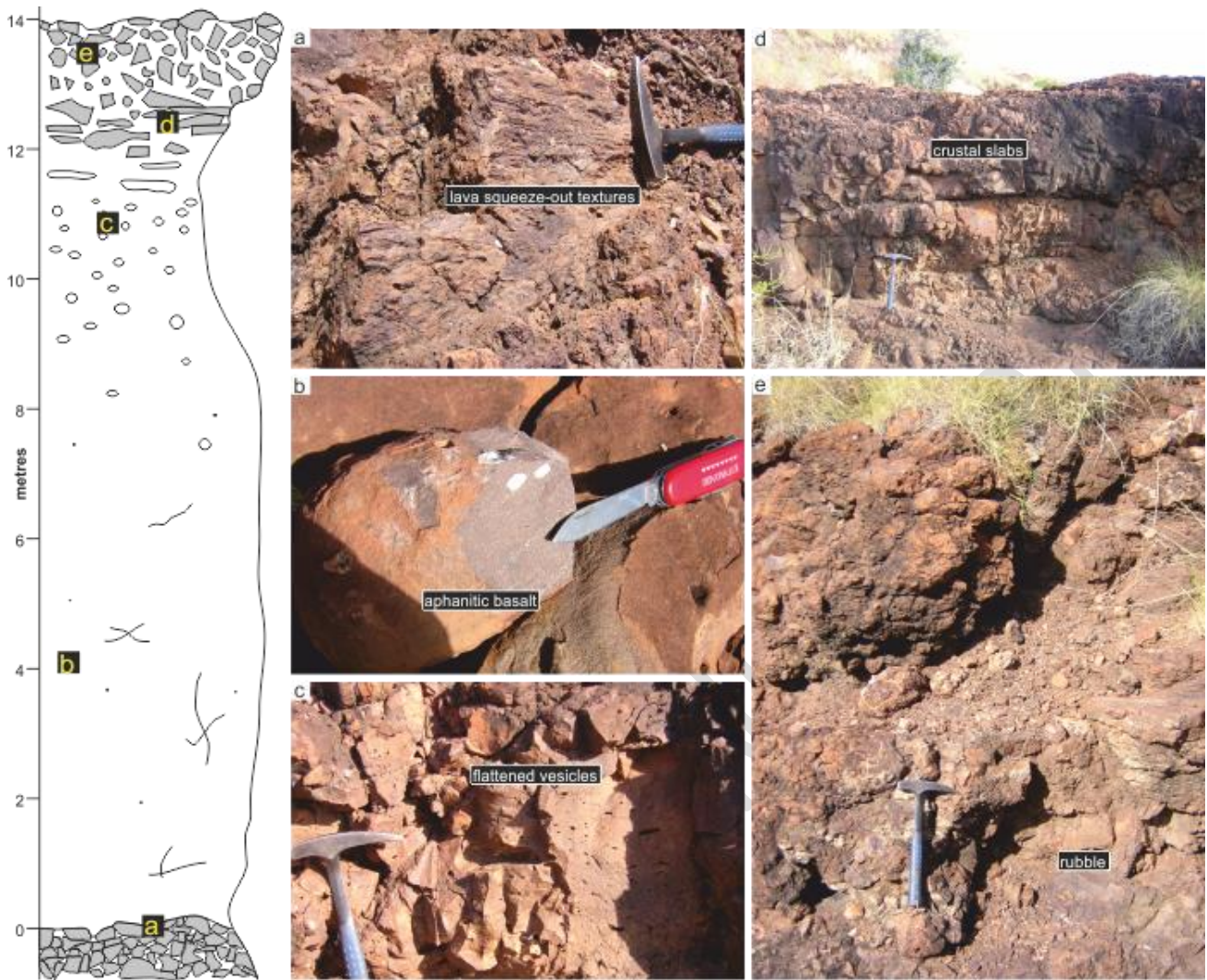
Figure 5: Summary log and field photographs from ouctrops in Purnululu National Park. a) Slabs of rubbly pāhoehoe from the flow below, displaying lava squeeze out textures. b) Aphanitic fine grained basaltic core. c) Vesicles collected at the core-top boundary. d) Disjointed horizontal plates at the top of flows weathering above the dipped flow cores. e) X-section of flow top comprising randomly assorted rubble.

2.3. South Ord Basin (DCBD & DCNN)

South of the Ord basin, the BRM succession crops out as a series of canyon cliffs cut by minor local rivers: two locations, 5 km apart, are separated by a N-S striking fault (associated with the margin of the nearby basin) giving a c. 60 m vertical displacement. At locality DCBD two near flat lying units may be identified, the core of the uppermost unit crops out at the roadside, with the lower unit well exposed in the canyon; the core to this lower unit forms the riverbed and the cliff immediately above provides excellent access to its thick rubble top. Both cores are grey coloured aphanitic-aphyric basalt with no internal structures evident. A thin layer of

vesicular material (<50 cm) marks the onset of this transition from core into the thick (c. 12 m) rubbly flow top; here the vesicles are spherical and evenly dispersed throughout the layer. At the core-top boundary the matrix is basaltic material, showing interactions with the clasts. The thick rubble above consists of jumbled blocks/clasts of highly vesicular scoria (10 – 30 cm diameter) set within a smaller, fragmental basalt matrix-supported breccia (Fig. 6a). Interestingly, the matrix found within the topmost 3 – 4 m of the rubble consists of well-sorted sub-rounded quartz sand grains.
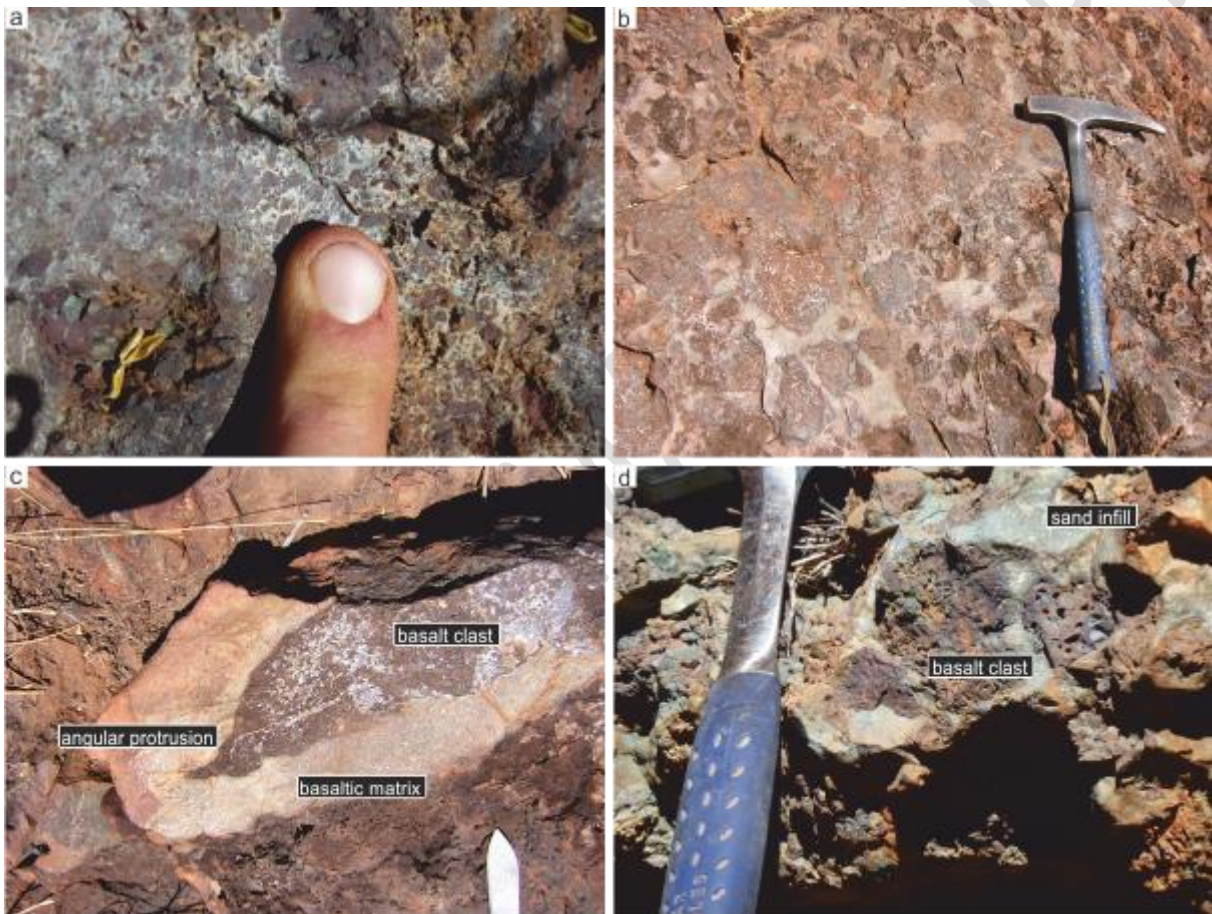

Figure 6: Field photographs of BRM outcrops at DCNN and DCBD. a) Small scale fragmental basalt matrix-supported breccia. b) Large basaltic blocks (>20 cm) forming a highly brecciated unit. c) A breccia with thin angular protrusions, indicative of lava extrusion not explosive tephra. d) Flow top breccia cemented together in a sand matrix.

Further south at DCNN two flows are similarly evident; the lower flow top crops out at the roadside with the core of the overlying flow forming a hillock 100 m west of the road. Core material is uniformly grey coloured, aphanitic basalt; the underlying flow top consists of large blocks of basaltic material forming a highly brecciated unit (Fig. 6b). These blocks consist of various crustal material including scoria, vesicular pods, and obvious fragments of pāhoehoe flow toes. In some instances the blocks display delicate extrusive features such as thin angular protrusions (Fig. 6c) and jig-saw type fracture patterns formed through cooling contraction, indicating minimal movement or disturbance during emplacement; such features are unlikely to be preserved in explosive tephra. This breccia appears to originally have had a very open structure and this, as at the previous location, is infilled with quartz sand (Fig. 6d).

2.4. North Ord Basin (DCSP, DCSS & DCWD)

The BRM crops out here as a series of N-S trending, 50 – 100 m high ridges rising immediately west of a 7 km long segment of the highway (16°45'31.3"S, 128°54'09.9"E - 16°49'11.4"S, 128°53'09.3"E). The upper, steep slopes consist of 3 or 4 very thick (>25 m), rubble topped flow units (Fig. 7a); the thickest of these forms a capping unit which has been dissected into a series of steep-sided, cliff-like mesas linked by narrow cols, whilst similar material forms block debris fields which cover the slopes below. Since access to the hill summits was difficult, fallen debris blocks (>5 m) were inspected and proved to be of similar composition to those as described at the previous localities. Samples were taken from in-situ flow cores exposed on lower slopes beneath the rubble debris (Fig. 7b).

Figure 7: Field photographs of BRM outcrops at DCWD and DCSS. a) Inaccessible hills displaying a series of flat-lying lava flows with the rubble tops weathered proud (highlighted by arrows). b) Large road-side outcrop of rubbly basalt flow core, beneath a rubble carapace topping the ridge.

Figure 8: Field photographs of BRM-like outcrops of vesiculated pods in a fine basaltic matrix observed at a) Blackfellow Creek (N1) and b) Biri Hill (BTBH).

2.5. Other observed occurrences of BRM-like outcrops

Several other outcrops were found beyond the mapped extent of the BRM around the Ord Basin and display

strikingly similar textured and internal structure.

2.5.1. North-West APV (N1)

A series of low basalt mesas (~100 m high) occur in the north west of the province. These are the most

northerly outcrops of basalt in the west of the APV and lie 143 km NNE of the type locality. The highest of

these hills (229 m a.s.l.) is capped by a thick rubble-topped unit. Clark (2014) describes this flow as 74 m of

continuous massive, melanocratic, fine- to medium-grained aphyric basalt, with poorly developed columnar

jointing towards the base. The unit's base consists of a thin veneer (<2 m) of undisrupted microcrystalline

basalt indicative of a basal chilled margin. The unit overlies basement quartz arenites. Vesicular basalt pods cluster at the core-breccia cap boundary. The flow top (> 10 m) is brecciated with clasts of vesicular and microcrystalline basalt set in a glassy microcrystalline basaltic matrix (Fig. 8a).

2.5.2. South-East APV (BTBH)

In the south east of the APV, the basalt has been eroded to a thin veneer of basalt with exposed inliers of Proterozoic basement. Thicker successions are preserved as rare, isolated mesas such as Biri Hill (BTBH), rising 80 m higher than the surrounding basalt. This mesa is capped by a 40 -50 m thick basaltic agglomerate similar to that observed at the localities described above (Fig. 8b): Clasts range in size from pebble (5 – 10 cm) to boulder (~ 50 cm), and massive basalt beneath poorly exposed in the lower slopes below.

2.5.3. Borehole (LB1)

LB1 lies at the southeastern edge of the Ord Basin, and was part of a comprehensive drilling survey of the APV (Bultitude, 1971). Analysis of drilling chips indicates that directly below 6.1 m of Headleys limestone the borehole intersects 4.5 m *(6.1 – 10.6 m)* of amygdaloidal basalt; this is taken to be the uppermost flow core of BRM. Below this *(10.6 – 32.0 m)* is 21.4 m of 85% agglomerate (dark-red, brown, heavily altered, mainly massive but often amygdaloidal), 15% sandstone (occurring as thin lenses scattered throughout the sequence) and then 36.6 m of 100% basalt *(32.0 – 68.6 m)*. These transitions between basalt, agglomerate and basalt below are interpreted as belonging to two units (c. 62.5 m) within the BRM.

2.5.4. - North-East APV (VCSP)

In the north east of the APV, basalt is seen to directly overlie Proterozoic sediments, the lowermost horizons in the basalt stratigraphy. Outcrop at the roadside appears blocky and rubbly; high amounts of weathering pick out gravel to boulder sized clasts and vesicular pods are prevalent throughout small mounds of rubbly flow top (S. Planke pers. comm.). This outcrop is furthest from the suspected source in the Ord Basin, and thus will represent the largest flows to have occurred in the APV.

2.6. Generalised flow structure of the BRM

All localities present the same general pattern of flow structure; this being laterally extensive, massive aphanitic grey coloured basaltic flow cores topped by a large thickness of agglomeratic rubble tops. Using these observations, a composite stratigraphical log (Fig. 9) may be assembled, and summarised as follows:

The flow core is 5 - 15 m thick with little or no internal vesiculation, thus indicating a nearly- or fully-degassed magma; these cores contain no evidence of rubble entrainment or basal crust (as may be expected from 'a'ā-type) forming an abrupt basal contact to the flow below.

At the top of the flow core sits a c. 1 - 2 m thick transition zone consisting of a variety of features associated with this physical junction between flow core and rubbly flow top. Preferential weathering reveals platy horizontal lineations which are inferred to be shear fabrics generated during emplacement and inflation of the molten core beneath a thick, insulating flow top breccia; this would have caused lava to freeze to the underside of rubble flow top leading to viscous shearing as lava flowed below. Beneath this 'shear zone' large horizontal gas blisters indicate a coalescence of gas bubbles at the top of the molten core, trapped beneath the solid crust above and spreading out along this boundary. Also at this boundary are vesicular pods, formed through extrusion and break-outs across the evolving surface of the flow; once cooled and solidified, this crust was broken up by continued flow disruption and brecciation, causing these vesicular fragments to become detached from the crust and re-entrained. With a high vesicle content, these pods would have been buoyant, hence their appearance within the upper section of molten core; once re-entrained these began to partially digest and re-assimilate into the lava core.

The rubble flow tops range from c. 15 - 20 m thickness and consist of randomly orientated, jumbled, highly vesicular and oxidised volcanic fragments. These are clearly derived from previous-pāhoehoe crust-forming episodes and range from gravel-sized scoria to boulder sized blocks which display a range of fragmental textures from angular crustal shards to sub-rounded boulders, indicating differential abrasion during movement and emplacement of the flow. Preserved in these blocks are characteristic crustal textures such as

flow ropes, vesiculated blocks and, despite considerable weathering and erosion of the APV, contain typical lava emplacement features such as pāhoehoe toes, slabby pāhoehoe, ropey surfaces and squeeze-outs. At the base of this rubbly lava top, these fragments and blocks of crust are matrix-supported by fine-grained basaltic groundmass; grading into a dominantly clast-supported breccia with only minor amounts of interstitial binding basaltic groundmass. It is within this layer that intrusive masses, rising as injections into the overlying rubble crust from the main flow core, may be identified; these are interpreted as lava protrusions and associated 'break-outs' that developed during inflation and broader lava emplacement process.
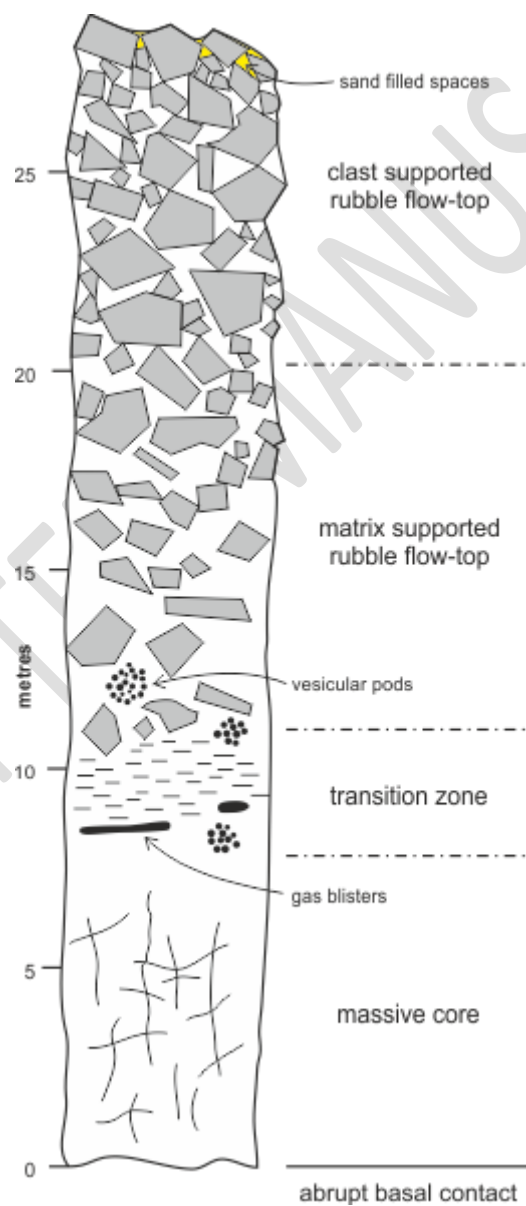

Figure 9: Summary stratigraphic log of the textures, features and morphologies observed in the Blackfella Rockhole Member (BRM).

Finally, as described earlier, the top of some of these giant rubble units contain arkosic sand which has infilled gaps between constituent clasts to form an interstitial matrix. This sand can be interpreted as either a wind-blown desert sand introduced and incorporated into the loose rubble flow top during periods of volcanic repose, or else derived from a strand-line or desert setting at the periphery of the province into which these lavas have flowed causing a peperite-style interaction (Jerram and Stollhofen, 2002). However, since no fluidal contacts or associated complex interaction between sand and lava were observed, such a peperite-type origin cannot be corroborated; instead these sands are here interpreted as sediment introduced to the lava flow top by rivers and/or aeolian processes acting across neo-formed lava fields during an eruptive hiatus.

3. Discussion

What becomes clear from these observations is that the interpretation of Mory & Beere (1985) concerning the BRM is essentially correct: the BRM units consist of a brecciated rubble top and an underlying massive basaltic inflation core, together comprising a single eruptive lava unit and not, as has been presumed by Evins et al. (2009) and Jourdan et al. (2014), as an explosive tephra.

3.1. Lava flow classification

The classification of a lava flow type is dependent upon the internal and surface morphology evident in the field. Pāhoehoe flows are the most common flow type in many CFBPs, and evolve as single inflation lobes that develop through endogenous filling to thicknesses of c. 10 - 20 m, thus presenting massive, undifferentiated flow cores (Self et al., 1998). By contrast, eruption units with brecciated flow tops and, crucially brecciated bases are termed 'a'ā flows. These are relatively uncommon in CFBP successions (Applegarth et al., 2010; Brown et al., 2011). Between these two end members, however, there is now an established and well-defined spectrum of genetically related lava types (Thordarson and Self, 1998; Single and Jerram, 2004; Brown et al.,

2011; Vye-Brown et al., 2013; Duraiswami et al., 2014). Where the flow is larger and more disturbed, 'slabby' pāhoehoe can be created by the rafting of large slabs into a jumble of tabular to curved pāhoehoe crusts disturbed, dislocated and tilted throughout the lava flow surface. Of importance to the current study are the more extreme forms within this spectrum of pāhoehoe crust disturbance – those which result in 'rubbly' pāhoehoe. Internally, these lavas consist of the usual large pāhoehoe inflation sheets, but are entirely covered with loose, brecciated blocks forming an agglomeratic breccia style flow top. Most importantly in all of these cases, the base of each flow consists of undisturbed pāhoehoe basalt and the clinker and autobrecciatiated material observed in 'a'ā lava bases is entirely absent.

The internal structure of the BRM is entirely consistent with rubbly pāhoehoe units described in Iceland and Columbia River (Guilbaud *et al.* 2005, 2007), though those of the BRM are significantly larger, both thicker (Kalkarindji: 25 - 40 m vs Laki: 7-10 m) and considerably more extensive - justly earning the appellation of 'giant rubbly flows' representing the last volcanic eruptions of the Kalkarindji CFBP. That the upper stratigraphy of the APV is exclusively rubbly pāhoehoe units, in contrast to lower sections where sheet pāhoehoe and compound lavas interleave with thin rubbly pāhoehoe units (Clark, 2014), indicates a significant shift in the nature of the eruptions toward the end of the Kalkarindji volcanic episode.

The two key questions arising from these observations are: 1) What caused the change from the typical CFBP pāhoehoe type inflation units, characteristic of the lower APV succession, to exclusively giant rubbly pāhoehoe BRM flows? 2) Since the BRM succession resulted from lava emplacement rather than phreatomagmatic activity could the eruptions of this specific lava type have had the effect upon the broader Cambrian environment suggested?

3.2. Emplacement style

There are several parameters known to affect lava rheology and generate a change from simple pāhoehoe inflation units to rubble-topped forms of the BRM. The morphology of a lava is dependent upon an interplay

between the key factors of viscosity and shear strain (Hon et al., 2003; Mader et al., 2013). Viscosity may be controlled by flow dimensions, lava crystallinity, dissolved gas content and vesicularity, temperature and flow velocity (which should be proportional to effusion rate and duration); the other key parameter, shear strain, can be controlled by environmentally-controlled parameters such as topography (ground slope and channel configuration) and the presence/interaction of water.

3.2.1. Flow dimensions

The size of extensive lava fields is either volume- or cooling-limited (Walker, 1973; Guest et al., 1987; Keszthelyi and Self, 1998); these factors determine the ancillary processes which play a key role in determining maximum extent. Our observations indicate that original areal extent of the BRM was smaller than that of the APV (< 100,000 km^2), yet large for a stack of rubble-topped flow fields (in excess of 15,000 km^2). Assuming an individual lava field is broadly lensoid in form (closely approximating to two broad cones joined at their bases), eruptive volume may be calculated by employing realistic estimates of minimum and maximum lava flow coverage and flow thicknesses (determined by field observation and interpolation of outcrop) by Eq. (1).

$$V = 2(A_v \frac{F_n F_h}{3}) \tag{1}$$

Where A_v is the area of lava coverage in km^2, F_n is the number of flows, and F_h is the flow thickness in km. Using this simple method, an estimated original area of 18,000 - 72,000 km^2 and 25 - 40 m thickness for the 5 - 10 BRM flows, a total eruptive volume of 1,500 km^3 – 19,200 km^3 may be estimated; this assumes a continuous lava field originating and hence centred in the Ord basin; a minimum coverage extending to the furthest reaches of the mapped unit and a maximum extent includes the further examples described in the east and north of the province (Fig. 3).

The inflation mechanism inherent in pāhoehoe flow fields of all scales (Hon et al., 1994; Self et al., 1997; 1998) provides a thermally efficient mechanism of lava transport through insulation of the internal lava flow by a thickened and cooled crust. Significantly, this insulation remains efficient whether the inflating flow is capped by a relatively undisturbed skin-like crust (pāhoehoe-type), or if it exhibits some degree of disruption (rubbly

pāhoehoe). By contrast, the considerable surface disruption, together with internal entrainment of crustal fragments characteristic of 'a'ā lava flows, results in thermally inefficient lava transport and, as a consequence, such flows are far less extensive. In the case of the BRM, the inflation model, and resulting generation of giant rubbly pāhoehoe flows, best explains how these lavas extended over 100s of km and indicates lava supply and volume was not a limiting factor of changes in viscosity.

3.2.2. Chemistry, crystallinity and vesicularity

Increases in silica and alumina content increase the degree of silicate polymerisation within a lava flow, thus resulting in higher viscosity. Accordingly, since the majority of the APV basalt succession is typical tholeiitic pāhoehoe flows, a difference in chemistry offers a likely cause of change to the rubbly pāhoehoe of the BRM. Such changes in chemistry are known to drive change in eruption dynamics and lava morphology (Bottinga and Weill, 1972). Analysis of 14 flow cores from different BRM localities were analysed for major and trace elements using least altered samples selected from the cores of the flows, all results are given in Table 2. Importantly, all BRM samples are of basaltic andesite composition and are chemically similar to other Kalkarindji lavas (Glass, 2002; Clark, 2014). Accordingly, since the BRM is chemically consistent with the majority of the Kalkarindji basalts, compositional change can be discounted as the main driver of viscosity and/or changes to eruption style (Fig. 10).

Increases in lava viscosity can also result from changes to the carried lava crystal load, or in the efficiency/degree of vesication (Truby et al., 2015). Changes to crystal load can result from increased groundmass crystallisation due to super-cooling (Guilbaud et al. 2007 and references therein), whilst variation in gas content or the rate of exsolution can affect vesiculation behaviour during lava emplacement. In both cases as either crystallinity and/or bubble content increases, basaltic lavas cease to behave as a Newtonian fluid (Lavallée et al., 2007), increasing in viscosity due to the reduced proportion of liquid volume; inducing internal rheological changes and thus causing a disruption to lava eruption and emplacement mechanisms (Chevrel et al., 2013; Mader et al., 2013).

Table 2: Major and trace element data for the BRM samples in this study.

Sample	BTBH-004	DCBD-001	DCBD-003	DCNN-004	DCSP-001	DCSS-001	DCWD-001	LB1-95-100	LB1-110-115	LB1-135-140	N1-005	NLRH-003	NLRH-006	NLRH-007	WS-E[a]	DNC-1[a]
Major elements (wt.%)																
SiO_2	54.62	55.32	52.67	52.45	52.12	53.16	56.21	50.69	56.11	53.93	54.10	53.24	55.76	54.97	51.57	-
TiO_2	1.21	1.63	1.31	1.31	0.85	1.27	1.09	1.71	1.57	1.30	1.24	1.50	1.71	1.75	2.42	-
Al_2O_3	14.32	13.60	13.78	13.67	14.72	13.84	14.19	14.82	13.71	13.68	14.14	14.06	13.12	13.37	13.95	-
Fe_2O_3T	12.26	13.45	12.37	12.44	9.38	12.07	10.01	13.90	12.89	12.68	12.04	8.15	14.04	13.50	13.16	-
MnO	0.16	0.14	0.20	0.20	0.14	0.18	0.14	0.24	0.20	0.20	0.15	0.08	0.18	0.17	0.17	-
MgO	5.04	3.74	5.71	5.46	7.64	5.08	4.63	8.17	4.87	5.80	5.19	3.09	3.07	3.33	5.53	-
CaO	7.92	6.92	6.38	5.93	7.38	6.18	6.35	1.02	4.53	5.16	8.16	6.68	6.24	4.53	8.92	-
Na_2O	2.68	2.37	3.61	1.73	3.73	3.19	3.39	4.18	2.73	3.49	3.05	3.84	2.65	3.13	2.41	-
K_2O	1.92	2.08	2.53	5.07	1.89	2.71	2.67	1.87	2.45	1.89	1.71	2.53	2.26	2.12	1.00	-
P_2O_5	0.15	0.17	0.14	0.14	0.10	0.14	0.15	0.19	0.18	0.15	0.12	0.16	0.19	0.18	0.30	-
L.O.I.	0.62	0.66	1.12	1.07	2.19	1.44	1.35	4.14	1.86	1.93	0.69	6.16	0.60	1.47	0.85	-
Total	100.90	100.08	99.83	99.46	100.14	99.25	100.19	100.93	101.11	100.16	100.61	99.48	99.81	98.53	100.28	-
FeO†	*11.03*	*12.10*	*11.13*	*11.19*	*8.44*	*10.86*	*9.01*	*12.51*	*11.60*	*11.41*	*10.83*	*7.33*	*12.63*	*12.15*	*11.84*	-
Trace elements (ppm)																
Cs	0.64	1.60	0.69	0.53	4.99	0.45	1.11	1.14	1.35	1.16	0.99	1.01	1.51	1.71	-	0.21
Rb	68.89	95.69	62.19	97.06	61.21	92.64	110.50	46.92	73.94	67.07	79.65	90.70	109.60	94.00	-	3.62
Ba	258.20	390.50	371.70	651.30	275.10	260.40	277.00	122.20	282.30	262.10	282.80	376.10	338.00	326.40	-	105
Th	8.66	13.62	6.97	7.48	5.99	9.94	12.31	13.95	13.29	9.88	8.94	12.67	14.89	15.26	-	0.25
U	1.39	2.17	1.16	1.23	0.81	1.53	2.13	2.43	2.20	1.58	1.48	2.08	2.54	2.62	-	0.06
Nb	8.09	11.26	6.66	7.01	6.14	9.87	10.22	13.41	11.69	9.33	7.54	10.89	13.46	12.52	-	1.68
Ta	0.85	0.82	0.50	0.54	2.02	2.82	2.36	4.02	0.88	0.67	0.55	0.76	2.04	1.13	-	0.29
La	20.78	30.58	18.65	19.70	15.57	23.44	26.68	25.10	29.52	23.58	20.75	59.52	35.32	39.43	-	3.73
Ce	42.18	62.13	37.68	39.85	31.55	46.81	53.63	58.28	59.97	48.04	42.01	81.32	70.48	70.49	-	8.14
Pb	6.90	11.88	7.66	8.38	6.77	9.18	10.63	3.17	12.16	12.71	10.88	8.34	14.84	17.27	-	5.95
Pr	5.10	7.40	4.61	4.87	3.84	5.61	6.32	7.24	7.23	5.78	5.08	9.16	8.33	8.18	-	1.10
Nd	19.77	27.71	18.07	19.15	14.75	21.27	23.50	27.89	27.12	22.02	19.63	34.95	30.98	31.19	-	4.92
Sr	134.95	143.20	334.15	715.65	253.20	242.55	153.40	63.56	136.40	127.15	161.60	114.80	190.75	120.20	-	143.40
Sm	4.79	6.31	4.43	4.69	3.51	4.96	5.31	6.66	6.20	5.18	4.72	7.55	6.93	6.93	-	1.42
Zr	136.60	185.05	132.65	142.15	106.00	152.25	161.75	201.30	189.40	154.65	131.35	179.40	209.45	198.20	-	35.51
Hf	3.63	4.82	3.48	3.72	2.77	4.00	4.19	5.20	4.91	3.97	3.41	4.78	5.29	5.32	-	0.98
Eu	1.23	1.52	1.26	1.33	0.98	1.29	1.27	1.67	1.49	1.27	1.27	2.01	1.63	1.69	-	0.59
Ti	7278	9883	8395	8691	5414	8060	6855	10540	9697	8325	8312	9257	11270	10360	-	2978
Gd	5.12	6.49	4.90	5.20	3.76	5.23	5.54	7.22	6.50	5.47	5.14	8.34	7.24	7.25	-	2.02
Tb	0.87	1.06	0.84	0.88	0.63	0.88	0.93	1.22	1.08	0.92	0.86	1.18	1.19	1.18	-	0.39
Dy	5.32	6.47	5.17	5.47	3.94	5.40	5.60	7.46	6.62	5.65	5.30	6.65	7.29	7.22	-	2.72
Ho	1.14	1.37	1.10	1.17	0.83	1.14	1.18	1.56	1.40	1.19	1.12	1.40	1.54	1.55	-	0.63
Y	33.97	40.96	32.23	34.42	24.53	34.12	35.43	48.25	41.56	36.01	33.43	43.16	47.58	44.14	-	18.54
Er	3.30	3.94	3.19	3.36	2.41	3.32	3.41	4.53	4.07	3.48	3.22	3.91	4.49	4.43	-	1.95
Yb	3.07	3.65	2.97	3.14	2.27	3.15	3.24	4.26	3.80	3.33	3.00	3.69	4.28	4.14	-	1.97
Lu	0.48	0.56	0.44	0.47	0.33	0.47	0.49	0.62	0.56	0.50	0.43	0.56	0.63	0.63	-	0.30
S	28.50	67.30	112.30	79.90	69.10	73.00	47.30	404.80	113.60	96.70	34.80	72.10	74.30	75.30	468.00	-

Concentrations of major elements were measured on fused glass beads by XRF and trace elements by acid dissolution ICP-MS at the Open University.
[a]Geochemical standards used for accuracy and precision.
†Calculated by multiplying through Fe_2O_3T by conversion factor of 0.8998.
Errors of <1 % for most major elements, and <5 % for most trace elements.

Primary volatile content is a fundamental control upon vesiculation. Low loss on ignition (LOI) values (Table 2) and the observation that the cores of BRM units are almost devoid of vesicles, indicate that near complete degassing occurred either at the vent source (Guilbaud et al., 2007) or during propagation across the evolving lava fields (Thordarson and Self, 1998). Effective degassing may be controlled by pre-eruptive (a magma with a long repose time or an initially low volatile content) or eruptive conditions (fire-fountaining at the vent source or slowing and stagnation of the flow). Evidence of vesiculation within the flow top indicates volatiles were still in the magma at time of eruption discounting an entirely degassed magma body. A low volatile content magma is more sensitive to change (Hess and Dingwell, 1996), magnifying the effects of degassing and the change in magma viscosity whilst slow lava propagation is more inclined to exhibit pāhoehoe textures, indicating a low volatile content induced rapid exsolution of gas in the conduit, increasing the lava flux and viscosity of the lava.
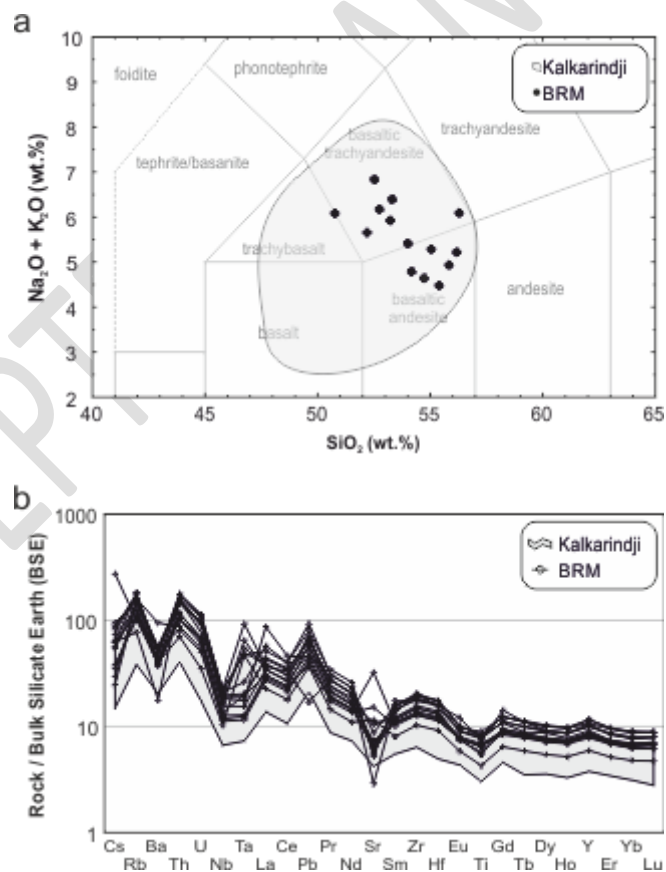

Figure 10: a) TAS (Total Alkali v Silica) diagram displaying the grouping of BRM samples to be basaltic andesites. b) Multi-element diagram displaying the grouping of BRM samples to lie at the upper end of the accepted bounds of a typical Kalkarindji sample. These plots indicate the lack of chemical variation from BRM to the majority of Kalkarindji.

3.2.3. Temperature

Inspection of thin sections from BRM lava cores reveal a groundmass of randomly orientated microcrystalline plagioclase laths (~70%), pyroxene (~15%) and opaques (magnetite, ilmenite and clays; ~15%). Small subhedral – anhedral plagioclase and clinopyroxene phenocrysts (0.5 – 2 mm) are present in some samples, but not abundant. Electron microprobe analysis (EMPA) of large plagioclase (> 1 mm) shows an average composition of $An_{56}Ab_{44}$, indicating an initial crystallisation temperature of ~1317 °C (at 0.1 MPa as originally defined by the experiments of Bowen 1913), whereas smaller plagioclase (0.5 - 1 mm) record a more sodic $An_{45}Ab_{55}$, showing secondary nucleation would have occurred around 1260 °C (at 0.1 MPa). Unfortunately, estimates of a final eruption temperature proved unobtainable because the microcrystalline groundmass is uniformly highly weathered.

Guilbaud et al. (2007) argue that magma super-cooling due to rapid degassing can initiate an increase in groundmass nucleation at high temperatures. The observed BRM plagioclase compositions better fit a model of two stage crystallisation: phenocryst nucleation during magma ascent at high temperatures, followed by rapid nucleation and crystallisation at lower eruption temperatures. The low amount of large (> 1 mm) phenocrysts and their relatively small size indicates a short time period between initial and secondary crystallisation. The abundance of fine grained (< 0.5 mm) groundmass crystals indicates rapid nucleation, possibly due to super-cooling. Applegarth et al. (2013) observed plagioclase growth pervasive up to 1250 °C at 1MPa when re-melting erupted basalts, following degassing at ~900 °C and proposed a threshold degree of degassing is required to drive super-cooled crystallisation. Whether this super-cooling occurred in the conduit (Melnik and Sparks, 2002) or as a delayed reaction in the BRM lavas (Lipman et al., 1985) is unknown.

3.2.4. Flow velocity

Eruptive mass effusion rate (the instantaneous volumetric flux of magma) is proportional to velocity and density of the erupting lava (Wadge, 1981). Temporally, this has been shown to increase rapidly from initial eruption, reaching maximum (waxing phase), before slowly decreasing with time until the cessation of

eruption (waning phase). Crucially, the length of time the flow stays at, or near to, maximum effusion rate will determine which lava morphology will form: during particularly high effusion rates basaltic lava can behave in a turbulent manner, resulting in channel-fed emplacement of rubble-dominated flows. Once effusion rate falls, tube-fed systems become increasingly well developed, and build widespread pāhoehoe and tumuli fields (Rowland and Walker, 1990). Given sufficient eruption duration and degree of tube extension, the pāhoehoe-tumuli field can eventually bury and extend beyond the initially emplaced 'a'ā field (Harris et al., 2007).

With no active measurement possible, determining an effusion rate for BRM-type eruptions requires modelling, with assumptions needed regarding likely viscosity, channel dimensions and topographic slope (Harris et al., 2007). Given the age and degree of erosion of the BRM, accurate parameterisation of these variables is problematic, whilst calculating an eruption rate (an average effusion rate across the entire eruption) requires a defined eruption duration, an unknown parameter without an effusion rate. Nevertheless, analogies may be made with the well-documented Laki eruption since it shares many common morphological and textural characteristics with BRM units and the Roza Member of the Columbia River Basalts due to a similar eruptive size (Table 3).

The 8 month-long fissure eruption at Laki produced a lava field covering 599 km^2 (Thordarson and Self, 1993) with a volume of 15.1 km^3 (Thordarson and Self, 2003); the Roza Member covers 40,300 km^2 with a volume of 1,300 km^3 (Tolan et al., 1989). Thordarson and Self (1993) consider that the unusual rubbly morphology of Laki resulted from sustained high effusion rates (up to 8700 m^3s^{-1}) and, arguably, this may also have been the case for those that fed the BRM flow fields and thus responsible for their distinctive architecture. If this analogy is correct, then the size of individual BRM flow fields must have been controlled by sustained high effusion and output volumes. Compared to Laki, a single BRM flow is estimated at between 300 km^3 - 1,920 km^3, a lava field 20 - 128 times larger than that erupted by Laki, and more comparable with the Roza Member, suggested to have erupted as a single 14 year event by Thordarson and Self (1998). Thordarson and Self (1998) calculated eruption duration and hence eruption rate in Columbia River based on the relationship between the thickness of a flow lobe and the conductive cooling rate (Hon et al., 1994); a simplistic model which requires a full section

of intact crust to measure, something not readily available in the BRM. However, Thordarson and Self (1993, 1998) found eruption rates of 2500 m^3s^{-1} are comparable between Laki and Roza despite the differences in size and morphology between the two flows, and thus a reasonable assumption can be made for these figures to apply also to the BRM given its similarities with both. The 27 km long Laki vent was erupted from 10 *en echelon* fissures (Thordarson and Self, 1993) whilst the vent complex of the Roza Member is known to be over 180 km long (Swanson et al., 1975; Brown et al., 2014), hence it is reasonable to suggest the as yet undiscovered vent structure of the BRM to be an order of magnitude larger than that of Laki, and thus able to produce significantly more lava at a similar rate akin to Roza.

With a constant effusion rate similar to those observed in Iceland, eruption duration of a single flow would have lasted 1 - 7 years. Assuming an average eruption rate of 2500 m^3s^{-1} when taking into account typical and expected lulls in magma supply and the waning of the effusion rate, a flow could have erupted over 4 - 24 years. Disregarding any potential hiatus between eruptive episodes, the total cumulative BRM eruption would likely have lasted anything between 19 - 244 years.

3.2.5. Syn-eruptive landscape topography

Another factor known to control basalt lava morphology is the syn-eruptive topography. Lava shear-strain increases with increasing topographic slope, accordingly, pāhoehoe lava of given viscosity seen to flow over steeper slopes ceases to act as a Newtonian fluid and instead shifts towards Bingham rheologies and 'a'ā style flows: such changes are readily observed as contemporary lava crosses the topography on the slopes of Mauna Loa (Peterson and Tilling, 1980; Hon et al., 2003). However, because such changes require local topographic variation, the change from pāhoehoe to 'a'ā and vice versa are restricted to the localised area where flow rate has been accelerated.

Changes in lava form are only rarely observed in CFBP successions (Guilbaud, 2006; Brown et al., 2011; Duraiswami et al., 2014) because early lava flows quickly fill and bury any pre-existing topography. Subsequently, the neo-formed lava fields present a broadly uniform, flat - gently undulose (variation over CFBP

lava surfaces is only of the order of 10s of metres, Jay et al. 2009), edaphically arid landscape to later lava encroachments. In the case of the BRM, the giant rubbly pāhoehoe units are clearly developed upon the earlier, extensive pāhoehoe dominated succession. Given the lateral continuity of these earlier lava fields, a lack of any evidence for erosion or development of significant topography between eruptive events and the fact that, in all but the peripheral zones, they were erupted onto this neo-formed stack of pāhoehoe units, we can assume that the syn-eruptive palaeo-landscape presented itself as a uniformly-flat topography to the advance of the later BRM flows.

The volcanic characteristics and structure of the unit at N1 are very similar to those observed at the type locality, but its unusual thickness probably indicates that lava had here become 'ponded' in a topographic low. If correct, then this outcrop is likely to represent an occurrence of BRM at the periphery of the APV, in a region which otherwise lay unaffected by all but the largest, most extensive of flows. Localised topographical differences would have resulted in transitions between lava types, however, even where the rubbly pāhoehoe persists as continuous outcrop for hundreds of metres, such variations are not observed. Rather the BRM succession consistently presents itself as a succession which may be correlated over 10s – 100s km. Therefore, topography or change of slope is unlikely to have been a significant contributor to the very widespread development of rubbly pāhoehoe.

3.2.6. Interactions with water

Interaction of water with lava is known to generate products ranging from changes in flow morphology, through to the development of pillow lavas and hyaloclastite deposits; impingement of the BRM flows into water bodies, or across a saturated substrate, may offer an explanation for the change to rubbly pāhoehoe dominated flow fields. Torsvik and Cocks (Torsvik and Cocks, 2009; Cocks and Torsvik, 2013) suggest the Kalkarindji CFBP erupted onto the periphery of the Gondwanan continent, thus introducing the possibility of marine influence upon syn-eruptive environments. Importantly, the APV sub-province is overlain by extensive stromatolitic limestones of late Cambrian age, indicating extensive post-eruptive epeiric flooding of the lava fields during the mid- to late Cambrian not long following the cessation of magmatic activity. In the east of the

province, near Biri Hill, the presence of patch reefs intercalated with the later levels of APV basalt stratigraphy (Beier et al., 2002) indicate that localised flooding, or development of restricted saline lakes had already occurred by the time of the BRM eruptions. Introduction of water might then explain the development of rubbly pāhoehoe as a product of water-lava interaction initiating a quenching of the crust, and subsequent autobrecciation of the flow. However, if lava-water interaction were the explanation for a change in lava morphology, then flooding would have had to have been widespread in order to account for the extensive coverage of the BRM flows. Other typical indicators of lava-water interaction such as peperite, hyaloclastites and pillow lavas are entirely absent from the observed outcrop, and all current observation indicates that these lavas were erupted into an unequivocally terrestrial environment.

Table 3: Comparison of physical characteristics and volatile emissions from Laki, Iceland (1773-1774), Roza Member, Columbia River (15 Ma) and the maximum and minimum calculated values for a single BRM flow.

Eruption	Laki	Roza Member	BRM [minimum]	BRM [maximum]
Area (km^2)	599 [a]	40,300 [d]	18,000	72,000
Volume (km^3)	15.1 [b]	1,300 [d]	300	1,920
Duration (years)	0.67 [a]	13.6 [e]	3.81	24.35
CO_2 (Tg)	3.04×10^2 [c]	1.43×10^4	3.30×10^3	2.11×10^4
CO_2/year (Tg a^{-1})	4.56×10^2	1.05×10^3	8.67×10^2	
SO_2 (Tg)	1.22×10^2 [b]	1.24×10^4 [f]	1.81×10^3	1.16×10^4
SO_2/year (Tg a^{-1})	1.83×10^2	1.20×10^3 [g]	4.76×10^2	

[a]Thordarson and Self (1993) [d]Tolan et al. (1989) [f]Thordarson and Self (1996)
[b]Thordarson and Self (2003) [e]Thordarson and Self (1998) [g]Self et al. (2006)
[c]Hartley et al. (2014)

3.3. Estimating total volatile release from the BRM

To address the second question raised concerning potential environmental impact, it is necessary to consider the quantity of volatiles (CO_2 and SO_2) released from the BRM during eruption. Both of these gases are present in significant quantities in basaltic magmas, and are known to alter atmospheric chemistry and the Earth's radiative balance.

We compare values for the BRM to those released from the modern-day and CFBP analogues - Laki and the Roza Member (Table 3), to aid in assessing any likely effect on Cambrian atmosphere and climate. As demonstrated here, the absence of widespread explosive tephritic material in the rock record leads to the assumption that these eruptions were relatively quiescent, with the only eruptive product being the rubbly pāhoehoe lavas seen today, hence the mass of these lavas was the main contributor to the volatile emissions.

3.3.1. Carbon dioxide (CO₂)

Direct measurement of CO_2 degassed during eruption of flood basalt magmas requires melt inclusions. This analysis is often not possible given the paucity of such inclusions in CFBP basalts and this together with the pervasive alteration of BRM samples precludes use of this method. Nevertheless, since CO_2 is relatively insoluble in basaltic melts, while the mantle is under-saturated with respect to CO_2 (Saal et al., 2002), we can employ values determined from previous estimates of CFBP volatile release (Self et al., 2005, 2006), and adopt 0.5 wt.% for the pre-eruptive CO_2 concentration in basalt. Assuming 100% degassing, the mass of CO_2 release can be calculated by Eq. (2):

$$M_{CO_2} = M_v\, C_{CO_2} \tag{2}$$

Where M_{CO_2} is the mass of CO_2 released from the molten lava in kg, M_v is the mass of magma in kg, and C_{CO_2} is the concentration of CO_2 in the melt as a mass fraction (0.005). The mass of basaltic magma can be determined by multiplying through density (2750 kg m^{-3}) with volume.

Since 100% efficient degassing is unrealistic, and the fact that gas was contained in the propagating BRM lavas (presence of gas blisters and vesicles), we assume ~80% CO_2 degassing as a reasonable estimate. Using the eruption volume estimates in Table 3, this would deliver 3.30×10^3 Tg – 2.11×10^4 Tg CO_2 during a single BRM eruptive episode. Assuming no hiatus between flows the whole BRM CO_2 output would total 1.65×10^4 Tg - 2.11×10^5 Tg at a rate of 8.67×10^2 Tg a^{-1}, compared with 3.15×10^4 Tg a^{-1} CO_2 produced annually from anthropogenic sources (Le Quéré et al., 2014). Given the modern atmosphere contains ~3×10^6 Tg CO_2 (Self et al., 2006), total instantaneous release from the entire BRM would increase CO_2 by up to 7%, however, since

the Cambrian atmosphere was around 15 times more enriched in background CO_2 (Crowley and Berner, 2001),

BRM CO_2 output in an theoretical instantaneous snapshot would contribute < 0.5% of the total atmospheric

CO_2 at the time of eruption. Laki emitted at least 3.04×10^2 Tg CO_2 (Hartley et al., 2014) whilst the Roza flow,

a single constituent of the Columbia River Basalts, contributed 1.43×10^4 Tg CO_2 (calculated by Eq. (2)) to the

Neogene atmosphere, a value similar to those estimated for the BRM. Neither Laki or Columbia River have

been correlated with any global mass extinction event (Bond and Wignall, 2014), therefore, the masses quoted

here effectively discounts the BRM alone from having had any significant long-term warming effect on global

atmospheric conditions.

3.3.2. Sulphur dioxide (SO_2)

Thordarson et al. (2003) and Self et al. (2005) detail a proxy method by which SO_2 volatile release may be

estimated from bulk geochemistry of crystal-poor lavas using the TiO_2/FeO ratio (Fig. 11a). Using a mean

TiO_2/FeO of 0.136, leads to an estimation for total S release of 0.11 wt.%. This value is corroborated by using

the simpler relationship between S solubility and Fe content of lavas via measured values (Fig. 11b). Using a

MORB array (Jenner and O'Neill, 2012) as proxy for melt inclusions within a primitive melt; a typical BRM melt,

given the low FeO content of the BRM lavas, would plot close to the S solubility line (~0.12 wt.% S), whereas

the measured values from BRM lava range from 0.003 - 0.04 wt.% S, inferring roughly 0.11 wt.% ΔS has been

lost through degassing. Using the lava volume estimates above and a compound ratio of 1.998 (converting S

to SO_2), this would have resulted in 1.81×10^3 Tg - 1.16×10^4 Tg total SO_2 released from a single BRM lava flow.

The Laki eruption lasted for 8 months, produced 1.22×10^2 Tg SO_2 (Thordarson et al., 1996) and affected global

climate for up to 2 years after cessation of the eruption because of the relatively quick (~1 year) buffering of

SO_2 and H_2SO_4 in the troposphere (Stevenson et al., 2003). A BRM lava flow lasting up to 24 years emitting SO_2

at a rate of 4.76×10^2 Tg a^{-1} could potentially effect environmental change if the delivery to the atmosphere

was efficient, yet evidence is scarce of any lasting damaging effects from the Columbia River Basalts where

the Roza flow produced 1.24×10^4 Tg SO_2 (Thordarson and Self, 1996) at a rate of 1.20×10^3 Tg a^{-1} (Self et al.,
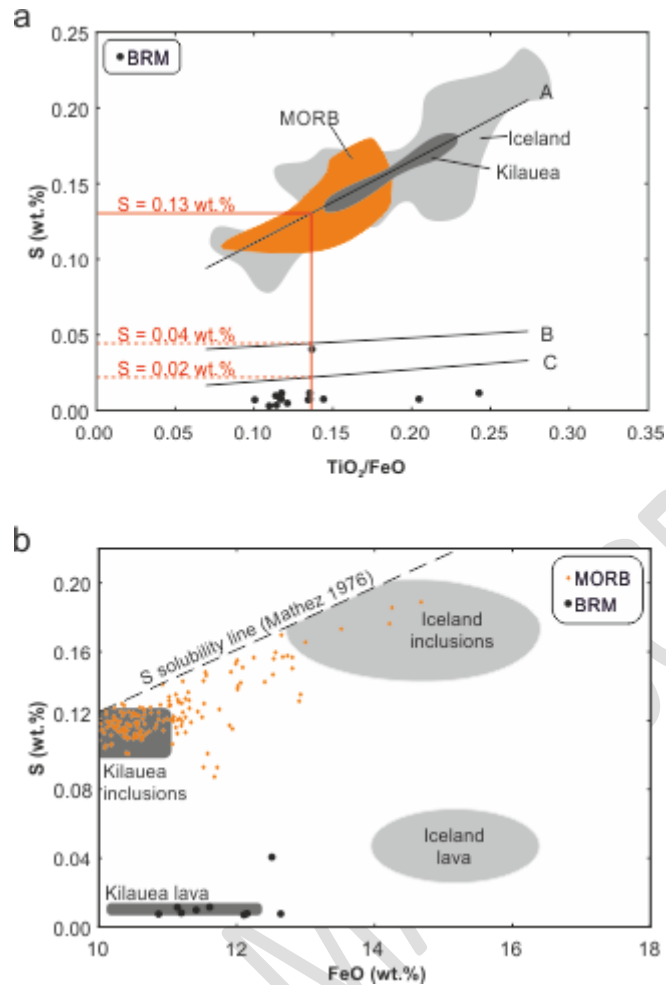
2006) over 14 years.

Figure 11: a) TiO2/FeO-S plot, displaying the prediction of S release from volcanic eruptions. Using the empirical relationship between S and TiO2/FeO ratio original S content of undegassed magma can be predicted by measuring the TiO2/FeO content of degassed erupted lavas. ABC lines of best fit based on observations from Kilauea, Iceland and MORB. A = sulphur in undegassed magma, B = sulphur contained in tephra after vent degassing, C = sulphur in lavas following degassing. A calculation of A-C gives an estimation of total ΔS. b) FeO-S plot, displaying the ΔS (wt.%) between a MORB proxy and BRM lavas in comparison with data fields for Iceland and Kilauea. (Both plots adjusted after Self et al., 2005; 2006; Data for Iceland and Kilauea noted in references in Self et al., 2006). S, TiO2 and FeO measured by XRF at the Open University, see Table 2. (MORB data taken from Jenner and O'Neill, 2012; S solubility line calculated by Mathez, 1976).

The effectiveness of volcanic SO_2 release as a driver for environmental change is dependent upon the mass delivered, the level in the atmosphere at which it is introduced and its atmospheric residence time. The most significant cooling effects occur when SO_2 is injected at stratospheric levels where its interactions cause significant increase in atmospheric optical density. It has been both observed (Stothers et al., 1986) and modelled (Woods, 1993) that basaltic fissure eruptions typically produce relatively low (< 15 km) eruption columns, confining atmospheric injection of volatiles to the upper troposphere and lowermost stratosphere where aerosol residence time is on the order of less than a year (Thordarson and Self, 2003). Basaltic fissure

eruptions at high latitudes (Iceland; 64°N) have the potential to reach stratospheric levels since the tropopause is relatively low (~ 9 km; Gettelman et al. 2002). In contrast, Kalkarindji was erupted near the equator (Torsvik and Cocks, 2009; Cocks and Torsvik, 2013) where the tropopause is at a greater altitude (~ 17km). Whilst an equatorial location would have aided in allowing aerosol distribution to both hemispheres, the restricted plume elevation and higher tropopause mitigate against stratospheric penetration, inhibiting global distribution of aerosols and the efficacy of individual BRM eruptions to affect global atmospheric conditions.

4. Conclusions

The Blackfella Rockhole Member is a series of simple giant rubble-topped inflation pāhoehoe sheet flows, which although limited examples have been noted in other provinces, are quite atypical of CFBP eruptions. These were emplaced in the final phase of the Kalkarindji CFB eruptions in the mid Cambrian, with an estimated original areal extent of 18,000 - 72,000 km^2 and total volume of 1,500 - 19,200 km^3, individual constituent lava fields are of the order of 300 - 1,920 km^3. Their emplacement represents a fundamental change in eruption style from earlier eruptions of more typical pāhoehoe and thin rubbly pāhoehoe lava, characteristic of the lower Kalkarindji succession. The closest modern analogue to these flows are from Laki, Iceland (Guilbaud et al., 2005) and even rarer examples documented in CFBPs from Columbia River (Guilbaud, 2006) and Deccan (Duraiswami et al., 2008, 2014).

Having considered the main rheological controls of flow dimension, lava crystallinity, dissolved volatile content, temperature, effusion rate, topography and lava-water interactions it is clear that external controls to shear strain were unlikely to have caused major variance in eruption style. The most dominant control to the development of the BRM lavas is an increased viscosity resulting from an interplay of low volatile content, and a high effusion rate sustained over a long period. The pre-eruptive conditions of volatile exsolution increased vesicularity as magma rose to the surface creating a more disturbed fluid in the conduit, causing rapid eruption of the BRM lavas. A flow would initiate as fast moving pāhoehoe with a rapidly solidifying crust

(Fig. 12a). Sustained high lava flux overwhelmed and disrupted the original crust generating a clinkered surface of squeeze-outs, broken blocks, slabs and rafts (Fig. 12b). Initially, this rapid moving lava would have entrained any remaining exsolved volatiles not degassed at/near the vent; these would then coalesce and collect beneath the thick rubble crust. As lava continued to be introduced into the flow at a high rate, the disrupted crustal slabs began to break up causing brecciation at the surface. At the core-top interface, autobrecciation of blocks and vesicular pods added to the thickening of the crust (Fig. 12c). These flows would propagate to an extent defined by the thickness of the overlying crust - the point where the weight of the overlying clinker can no longer be supported by the relatively thin core. Break-outs may occur and feed new flow lobes. Termination of flow propagation caused lava to back up, inflating the flow in a similar fashion to a simple pāhoehoe flow, creating the giant rubble crusts of BRM rubbly pāhoehoe lavas with relatively thin flow cores (Fig. 12d).

Cumulatively the BRM eruptions lasted, at the very minimum lasted for ~ 20 years and potentially much longer although expected volcanic hiatuses mean this was unlikely to have been concurrent. Sulphur (~ 2.5 times as much as that delivered by Laki) was constantly being replenished in the troposphere every year of eruption, however this was far below that emitted by the similarly sized Roza Member. Intriguingly, the much more voluminous Columbia River Basalts are not correlated with any known global environmental catastrophe in the Neogene. Therefore, considering the size, volumes and masses involved during lava emplacement, we conclude that even though erupted into a fragile ecosystem, with low biodiversity at the dawn of the Phanerozoic, the BRM eruptions alone are unlikely to have had a major global effect on the Cambrian environment.
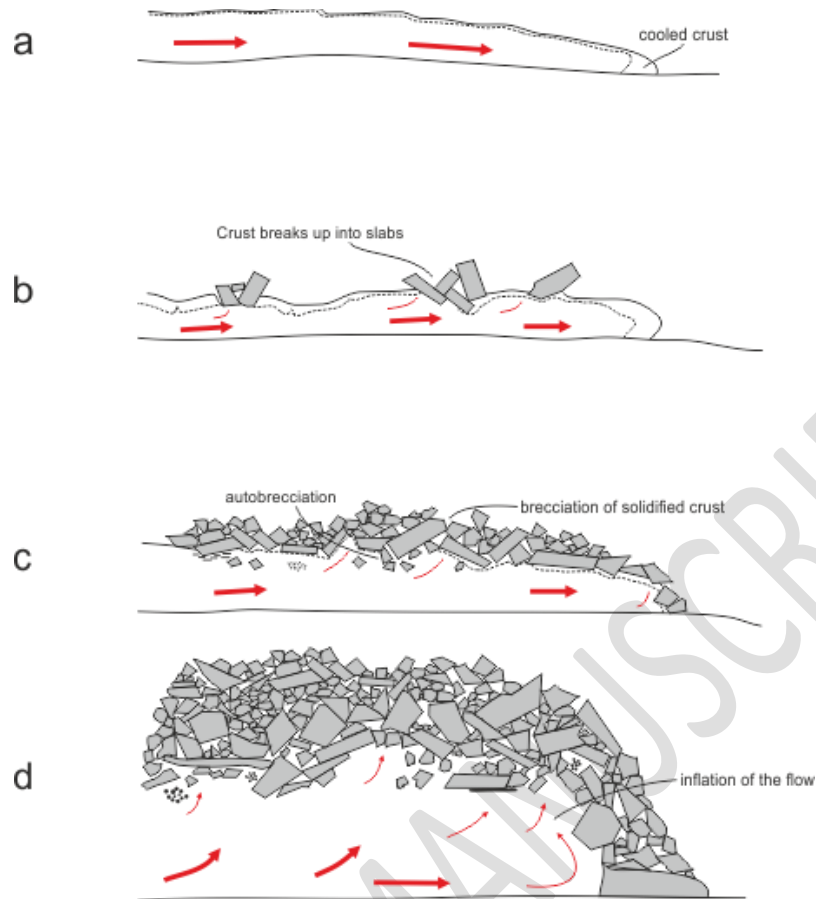
Figure 12: Schematic representation of the mode of emplacement of giant rubbly pāhoehoe lava. a) Initial extrusion of a simple pāhoehoe is fast owing to high effusion rates. The crust begins to quickly cool. b) Continued fast influx of a more viscous lava disrupts and ruptures the crust into slab which stack on top of the flow. c) Brecciation of these slabs on the surface builds a thickening clinker carapace on the surface of the flow. Autobrecciation at the core-top interface thickens the crust downwards. Vesicular pods also collect at this boundary. d) When the flow can no longer support the overlying crust, inflation of the flow lobe occurs, generating giant rubbly pāhoehoe.

Acknowledgements

Appendix. Supplementary Material

Supplementary material for this article can be found online at

http://dx.doi.org/10.1016/j.palaeo.2015.05.006.

References

Applegarth, L.J., Pinkerton, H., James, M.R., Calvari, S., 2010. Morphological complexities and hazards during the emplacement of channel-fed 'a'ā lava flow fields: A study of the 2001 lower flow field on Etna. Bull. Volcanol. 72, 641–656. http://dx.doi.org/10.1007/s00445-010-0351-1.

Applegarth, L.J., Tuffen, H., James, M.R., Pinkerton, H., Cashman, K. V., 2013. Direct observations of degassing-induced crystallization in basalts. Geology 41, 243–246. http://dx.doi.org/10.1130/G33641.1.

Beier, P.R., Dunster, J.N., Cutovinos, A., Pietsch, B.A., 2002. Victoria River Downs, Northern Territory (Second Edition), 1:250 000 geological map series and explanatory notes, SE 52-4. Northern Territory Geological Survey, Darwin.

Bond, D.P.G., Wignall, P.B., 2014. Large igneous provinces and mass extinctions: An update. Geol. Soc. Am. Spec. Pap. 505, 29–55. http://dx.doi.org/10.1130/2014.2505(02).

Bondre, N.R., Duraiswami, R.A., Dole, G., 2004. Morphology and emplacement of flows from the Deccan Volcanic Province, India. Bull. Volcanol. 66, 29–45. http://dx.doi.org/10.1007/s00445-003-0294-x.

Bottinga, Y., Weill, D.F., 1972. The Viscosity of Magmatic Silicate Liquids: A Model for Calculation. Am. J. Sci. 272, 438–475. http://dx.doi.org/10.2475/ajs.272.5.438.

Bowen, N.L., 1913. The melting phenomena of the Plagioclase Feldspars. Am. J. Sci. 35, 577–599. http://dx.doi.org/10.2475/ajs.s4-35.210.577.

Brown, R.J., Blake, S., Bondre, N.R., Phadnis, V.M., Self, S., 2011. ´A´ā lava flows in the Deccan Volcanic Province, India, and their significance for the nature of continental flood basalt eruptions. Bull. Volcanol. 73, 737–752. http://dx.doi.org/10.1007/s00445-011-0450-7.

Brown, R.J., Blake, S., Thordarson, T., Self, S., 2014. Pyroclastic edifices record vigorous lava fountains during the emplacement of a flood basalt flow field, Roza Member, Columbia River Basalt Province, USA. Geol. Soc. Am. Bull. 1–17. http://dx.doi.org/10.1130/B30857.1.

Bryan, S.E., Peate, I.U., Peate, D.W., Self, S., Jerram, D.A., Mawby, M.R., Marsh, J.S. (Goonie), Miller, J.A., 2010. The largest volcanic eruptions on Earth. Earth-Science Rev. 102, 207–229. http://dx.doi.org/10.1016/j.earscirev.2010.07.001.

Bultitude, R.J., 1976. Flood basalts of probable early Cambrian age in northern Australia, in: Johnson, R.W. (Ed.), Volcanism in Australasia. Canberra, pp. 1–20.

Bultitude, R.J., 1972. The Geology and Petrology of the Helen Springs, Nutwood Downs, and Peaker Piker Volcanics. Bur. Miner. Resour. Geol. Geophys. 1972/74.

Bultitude, R.J., 1971. The Antrim Plateau Volcanics, Victoria River District, Northern Territory. Bur. Miner. Resour. Geol. Geophys. 1971/69.

Chevrel, M.O., Platz, T., Hauber, E., Baratoux, D., Lavallée, Y., Dingwell, D.B., 2013. Lava flow rheology: A comparison of morphological and petrological methods. Earth Planet. Sci. Lett. 384, 109–120. http://dx.doi.org/10.1016/j.epsl.2013.09.022.

Clark, N., 2014. Volcanic Architecture and Chemostratigraphy within the Kalkarindji Continental Flood Basalt Province, Northern Territory: Implications for eruption style from multiple fissure eruptions. MSc. Thesis. Queensland University of Technology.

Cocks, L.R.M., Torsvik, T.H., 2013. The dynamic evolution of the Palaeozoic geography of eastern Asia. Earth-Science Rev. 117, 40–79. http://dx.doi.org/10.1016/j.earscirev.2012.12.001.

Coffin, M.F., Eldholm, O., 1994. Large igneous provinces: crustal structure, dimensions, and external consequences. Rev. Geophys. 32, 1–36. http://dx.doi.org/10.1029/93RG02508.

Crowley, T.J., Berner, R.A., 2001. CO2 and Climate Change. Science 292, 870–872. http://dx.doi.org/10.1126/science.1061664.

Cutovinos, A., Beier, P.R., Kruse, P.D., Abbot, S.T., Dunster, J.N., Brescianini, R.F., 2002. Limbunya, Northern Territory (Second Edition), 1:250 000 geological map series and explanatory notes, SE 52-07. Northern Territory Geological Survey, Darwin and Alice Springs.

Dow, D.B., 1980. Palaeozoic Rocks of the Hardman, Rosewood, and Argyle Basins, East Kimberley Region, Western Australia. Bur. Miner. Resour. Geol. Geophys. 1980/54.

Dow, D.B., Gemuts, I., Plumb, K.A., Dunnet, D., 1964. The Geology of the Ord River Region, Western Australia. Bur. Miner. Resour. Geol. Geophys. 1964/104.

Duraiswami, R.A., Bondre, N.R., Managave, S., 2008. Morphology of rubbly pahoehoe (simple) flows from the Deccan Volcanic Province: Implications for style of emplacement. J. Volcanol. Geotherm. Res. 177, 822–836. http://dx.doi.org/10.1016/j.jvolgeores.2008.01.048.

Duraiswami, R.A., Gadpallu, P., Shaikh, T.N., Cardin, N., 2014. Pahoehoe–a'a transitions in the lava flow fields of the western Deccan Traps, India-implications for emplacement dynamics, flood basalt architecture and volcanic stratigraphy. J. Asian Earth Sci. 84, 146–166. http://dx.doi.org/10.1016/j.jseaes.2013.08.025.

Duraiswami, R.A., Bondre, N.R., Dole, G., Phadnis, V.M., Kale, V.S., 2001. Tumuli and associated features from the western Deccan Volcanic Province, India. Bull. Volcanol. 63, 435–442. http://dx.doi.org/10.1007/s004450100160.

Ernst, R.E., Bleeker, W., Söderlund, U., Kerr, A.C., 2013. Large Igneous Provinces and supercontinents: Toward completing the plate tectonic revolution. Lithos 174, 1–14. http://dx.doi.org/10.1016/j.lithos.2013.02.017.

Ernst, R.E., Wingate, M.T.D., Buchan, K.L., Li, Z.X., 2008. Global record of 1600–700 Ma Large Igneous Provinces (LIPs): Implications for the reconstruction of the proposed Nuna (Columbia) and Rodinia supercontinents. Precambrian Res. 160, 159–178. http://dx.doi.org/10.1016/j.precamres.2007.04.019.

Evins, L.Z., Jourdan, F., Phillips, D., 2009. The Cambrian Kalkarindji Large Igneous Province: Extent and characteristics based on new $^{40}Ar/^{39}Ar$ and geochemical data. Lithos 110, 294–304. http://dx.doi.org/10.1016/j.lithos.2009.01.014.

Foden, J., Elburg, M.A., Dougherty-Page, J., Burtt, A., 2006. The Timing and Duration of the Delamerian Orogeny: Correlation with the Ross Orogen and Implications for Gondwana Assembly. J. Geol. 114, 189–210. http://dx.doi.org/10.1086/499570.

Gettelman, A., Salby, M.L., Sassi, F., 2002. Distribution and influence of convection in the tropical tropopause region. J. Geophys. Res. 107, 4080. http://dx.doi.org/10.1029/2001JD001048.

Glass, L.M., 2002. Petrogenesis and Geochronology of the North Australian Kalkarinji Low-Ti Continental Flood Basalt Province. PhD. Thesis. Australian National University.

Glass, L.M., Phillips, D., 2006. The Kalkarindji continental flood basalt province: A new Cambrian large igneous province in Australia with possible links to faunal extinctions. Geology 34, 461–464. http://dx.doi.org/10.1130/G22122.1.

Grey, K., Hocking, R.M., Stevens, M.K., Bagas, L., Carlsen, G.M., Irimies, F., Pirajno, F., Haines, P., Apak, S.N., 2005. Lithostratigraphic nomenclature of the Officer Basin and correlative parts of the Paterson Orogen, Western Australia, Geological Survey of Western Australia. Rep. 93, 89.

Guest, J.E., Kilburn, C.R.J., Pinkerton, H., Duncan, A.M., 1987. The evolution of lava flow-fields: observations of the 1981 and 1983 eruptions of Mount Etna, Sicily. Bull. Volcanol. 49, 527–540. http://dx.doi.org/10.1007/BF01080447.

Guilbaud, M.-N., 2006. The Origin of Basaltic Lava Flow Textures. PhD. Thesis. The Open University.

Guilbaud, M.-N., Blake, S., Thordarson, T., Self, S., 2007. Role of Syn-eruptive Cooling and Degassing on Textures of Lavas from the AD 1783-1784 Laki Eruption, South Iceland. J. Petrol. 48, 1265–1294. http://dx.doi.org/10.1093/petrology/egm017.

Guilbaud, M.-N., Self, S., Thordarson, T., Blake, S., 2005. Morphology, surface structures, and emplacement of lavas produced by Laki AD 1783-84. Geol. Soc. Am. Spec. Pap. 396, 81–102. http://dx.doi.org/10.1130/0-8137-2396-5.81.

Hanley, L.M., Wingate, M.T.D., 2000. SHRIMP zircon age for an Early Cambrian dolerite dyke: An intrusive phase of the Antrim Plateau Volcanics of northern Australia. Aust. J. Earth Sci. 47, 1029–1040. http://dx.doi.org/10.1046/j.1440-0952.2000.00829.x.

Harris, A.J.L., Dehn, J., Calvari, S., 2007. Lava effusion rate definition and measurement: a review. Bull. Volcanol. 70, 1–22. http://dx.doi.org/10.1007/s00445-007-0120-y.

Hartley, M.E., Maclennan, J., Edmonds, M., Thordarson, T., 2014. Reconstructing the deep CO_2 degassing behaviour of large basaltic fissure eruptions. Earth Planet. Sci. Lett. 393, 120–131. http://dx.doi.org/10.1016/j.epsl.2014.02.031.

Hess, K.U., Dingwell, D.B., 1996. Viscosities of hydrous leucogranitic melts: A non-Arrhenian model. Am. Mineral. 81, 1297–1300.

Hon, K., Gansecki, C., Kauahikaua, J., 2003. The transition from "a"ā to pāhoehoe crust on flows emplaced during the Pu'u "Ō"ō-Kūpaianaha eruption., in: USGS Prof. Paper 1676. pp. 89–103.

Hon, K., Kauahikaua, J., Denlinger, R., Mackay, K., 1994. Emplacement and inflation of pahoehoe sheet flows: Observations and measurements of active lava flows on Kilauea Volcano, Hawaii. Geol. Soc. Am. Bull. 106, 351–370. http://dx.doi.org/10.1130/0016-7606(1994)106<0351.

Jay, A.E., Niocaill, C.M., Widdowson, M., Self, S., Turner, W., 2009. New palaeomagnetic data from the Mahabaleshwar Plateau, Deccan Flood Basalt Province, India: implications for the volcanostratigraphic architecture of continental flood basalt provinces. J. Geol. Soc. London. 166, 13–24. http://dx.doi.org/10.1144/0016-76492007-150.

Jenner, F.E., O'Neill, H.S.C., 2012. Analysis of 60 elements in 616 ocean floor basaltic glasses. Geochemistry, Geophys. Geosystems 13, Q02005. http://dx.doi.org/10.1029/2011GC004009.

Jerram, D.A., Stollhofen, H., 2002. Lava–sediment interaction in desert settings; are all peperite-like textures the result of magma–water interaction? J. Volcanol. Geotherm. Res. 114, 231–249. http://dx.doi.org/10.1016/S0377-0273(01)00279-7.

Jerram, D.A., Widdowson, M., 2005. The anatomy of Continental Flood Basalt Provinces: geological constraints on the processes and products of flood volcanism. Lithos 79, 385–405. http://dx.doi.org/10.1016/j.lithos.2004.09.009.

Jourdan, F., Hodges, K., Sell, B., Schaltegger, U., Wingate, M.T.D., Evins, L.Z., Soderlund, U., Haines, P.W., Phillips, D., Blenkinsop, T., 2014. High-precision dating of the Kalkarindji large igneous province, Australia, and synchrony with the Early-Middle Cambrian (Stage 4-5) extinction. Geology 42, 543–546. http://dx.doi.org/10.1130/G35434.1.

Keszthelyi, L., Self, S., 1998. Some physical requirements for the emplacement of long basaltic lava flows. J. Geophys. Res. 103, 27447–27464. http://dx.doi.org/10.1029/98JB00606.

Lavallée, Y., Hess, K.-U., Cordonnier, B., Bruce Dingwell, D., 2007. Non-Newtonian rheological law for highly crystalline dome lavas. Geology 35, 843. http://dx.doi.org/10.1130/G23594A.1.

Le Quéré, C., Peters, G.P., Andres, R.J., Andrew, R.M., Boden, T.A., Ciais, P., Friedlingstein, P., Houghton, R.A., Marland, G., Moriarty, R., Sitch, S., Tans, P., Arneth, A., Arvanitis, A., Bakker, D.C.E., Bopp, L., Canadell, J.G., Chini, L.P., Doney, S.C., Harper, A., Harris, I., House, J.I., Jain, A.K., Jones, S.D., Kato, E., Keeling, R.F., Klein Goldewijk, K., Körtzinger, A., Koven, C., Lefèvre, N., Maignan, F., Omar, A., Ono, T., Park, G.-H., Pfeil, B., Poulter, B., Raupach, M.R., Regnier, P., Rödenbeck, C., Saito, S., Schwinger, J., Segschneider, J., Stocker, B.D., Takahashi, T., Tilbrook, B., Van Heuven, S., Viovy, N., Wanninkhof, R., Wiltshire, A., Zaehle, S., 2014. Global carbon budget 2013. Earth Syst. Sci. Data 6, 235–263. http://dx.doi.org/10.5194/essd-6-235-2014.

Lipman, P.W., Banks, N.G., Rhodes, J.M., 1985. Degassing-induced crystallization of basaltic magma and effects on lava rheology. Nature 317, 604–607. http://dx.doi.org/10.1038/317604a0.

Mader, H.M., Llewellin, E.W., Mueller, S.P., 2013. The rheology of two-phase magmas: A review and analysis. J. Volcanol. Geotherm. Res. 257, 135–158. http://dx.doi.org/10.1038/317604a0.

Mathez, E.A., 1976. Sulfur Solubility and Magmatic Sulfides in Submarine Basalt. J. Geophys. Res. 81, 4269–4276. http://dx.doi.org/10.1029/JB081i023p04269.

Melnik, O., Sparks, R.S.J., 2002. Dynamics of magma ascent and lava extrusion at Soufrière Hills Volcano, Montserrat. Geol. Soc. London, Mem. 21, 153–171. http://dx.doi.org/10.1144/GSL.MEM.2002.021.01.07.

Mory, A.J., Beere, G.M., 1988. Geology of the Onshore Bonaparte and Ord Basins in Western Australia. Geol. Surv. West. Aust. Bull. 134.

Mory, A.J., Beere, G.M., 1985. Palaeozoic Stratigraphy of the Ord Basin, Western Australia and Northern Territory. Geol. Surv. West. Aust. Artic. 14, 36–45.

Peterson, D.W., Tilling, R.I., 1980. Transition of Basaltic Lava from Pāhoehoe to "A"ā, Kilauea Volcano, Hawai'i: Field Observations and Key Factors. J. Volcanol. Geotherm. Res. 7, 271–293. http://dx.doi.org/10.1016/j.jvolgeores.2013.02.014.

Pirajno, F., Hoatson, D.M., 2012. A review of Australia's Large Igneous Provinces and associated mineral systems: Implications for mantle dynamics through geological time. Ore Geol. Rev. 48, 2–54. http://dx.doi.org/10.1016/j.oregeorev.2012.04.007.

Playford, P.E., Cope, R.N., Cockbain, A.E., Low, G.H., Lowry, D.C., 1975. Ord Basin, in: Geology of Western Australia: West. Australia Geol Survey, Memoir 2. pp. 395–399.

Ross, P.-S., Ukstins Peate, I., McClintock, M.K., Xu, Y.G., Skilling, I.P., White, J.D.L., Houghton, B.F., 2005. Mafic volcaniclastic deposits in flood basalt provinces: A review. J. Volcanol. Geotherm. Res. 145, 281–314. http://dx.doi.org/10.1016/j.jvolgeores.2005.02.003.

Rowland, S.K., Walker, G.P.L., 1990. Pahoehoe and aa in Hawaii: volumetric flow rate controls the lava structure. Bull. Volcanol. 52, 615–628. http://dx.doi.org/10.1007/BF00301212.

Saal, A.E., Hauri, E.H., Langmuir, C.H., Perfit, M.R., 2002. Vapour undersaturation in primitive mid-ocean-ridge basalt and the volatile content of Earth's upper mantle. Nature 419, 451–455. http://dx.doi.org/10.1038/nature01073.

Self, S., Keszthelyi, L., Thordarson, T., 1998. The Importance of Pāhoehoe. Annu. Rev. Earth Planet. Sci. 26, 81–110. http://dx.doi.org/10.1146/annurev.earth.26.1.81.

Self, S., Thordarson, T., Keszthelyi, L., 1997. Emplacement of continental flood basalt lava flows, in: Mahoney, J.J., Coffin, M.F. (Eds.), Large Igneous Provinces: Continental, Oceanic, and Planetary Flood Volcanism. American Geophysical Union, pp. 381–410.

Self, S., Thordarson, T., Widdowson, M., 2005. Gas Fluxes from Flood Basalt Eruptions. Elements 1, 283–287. http://dx.doi.org/10.2113/gselements.1.5.283.

Self, S., Widdowson, M., Thordarson, T., Jay, A.E., 2006. Volatile fluxes during flood basalt eruptions and potential effects on the global environment: A Deccan perspective. Earth Planet. Sci. Lett. 248, 518–532. http://dx.doi.org/10.1016/j.epsl.2006.05.041.

Sheth, H., Meliksetian, K., Gevorgyan, H., Israyelyan, A., Navasardyan, G., 2015. Intracanyon basalt lavas of the Debed River (northern Armenia), part of a Pliocene–Pleistocene continental flood basalt province in the South Caucasus. J. Volcanol. Geotherm. Res. 295, 1–15. http://dx.doi.org/10.1016/j.jvolgeores.2015.02.010.

Single, R.T., Jerram, D.A., 2004. The 3D facies architecture of flood basalt provinces and their internal heterogeneity: examples from the Palaeogene Skye Lava Field. J. Geol. Soc. London. 161, 911–926. http://dx.doi.org/10.1144/0016-764903-136.

Stevenson, D.S., Johnson, C.E., Highwood, E.J., Gauci, V., Collins, W.J., Derwent, R.G., 2003. Atmospheric impact of the 1783 – 1784 Laki eruption: Part I Chemistry modelling. Atmos. Chem. Phys. 3, 487–507. http://dx.doi.org/10.5194/acp-3-487-2003.

Stothers, R.B., Wolff, J.A., Self, S., Rampino, M., 1986. Basaltic fissure eruptions, plume heights, and atmospheric aerosols. Geophys. Res. Lett. 13, 725–728. http://dx.doi.org/10.1029/GL013i008p00725.

Swanson, D.A., Wright, T.L., Helz, R.T., 1975. Linear vent systems and estimated rates of magma production and eruption for the Yakima Basalt on the Columbia Plateau. Am. J. Sci. 275, 877–905. http://dx.doi.org/10.2475/ajs.275.8.877.

Sweet, I.P., Mendum, J.R., Bultitude, R.J., Morgan, C.M., 1974. The Geology of the Southern Victoria River Region, Northern Territory. Bur. Miner. Resour. Geol. Geophys. Report 167.

Sweet, I.P., Mendum, J.R., Bultitude, R.J., Morgan, C.M., 1971. The Geology of the Waterloo, Victoria River Downs, Limbunya and Wave Hill 1:250,000 Sheet Areas, Northern Territory. Bur. Miner. Resour. Geol. Geophys. 1971/71.

Thordarson, T., Self, S., 2003. Atmospheric and environmental effects of the 1783–1784 Laki eruption: A review and reassessment. J. Geophys. Res. 108, 4011. http://dx.doi.org/10.1029/2001JD002042.

Thordarson, T., Self, S., 1998. The Roza Member, Columbia River Basalt Group : A gigantic pahoehoe lava flow field formed by endogenous processes? J. Geophys. Res. 103, 27,411–27,445. http://dx.doi.org/10.1029/98JB01355.

Thordarson, T., Self, S., 1996. Sulfur, chlorine and fluorine degassing and atmospheric loading by the Roza eruption, Columbia River Basalt Group, Washington, USA. J. Volcanol. Geotherm. Res. 74, 49–73. http://dx.doi.org/10.1016/S0377-0273(96)00054-6.

Thordarson, T., Self, S., 1993. The Laki (Skaftár Fires) and Grímsvötn eruptions. Bull. Volcanol. 55, 233–263. http://dx.doi.org/10.1007/BF00624353.

Thordarson, T., Self, S., Miller, D.J., Larsen, G., Vilmundardottir, E.G., 2003. Sulphur release from flood lava eruptions in the Veidivotn, Grimsvotn and Katla volcanic systems, Iceland. Geol. Soc. London, Spec. Publ. 213, 103–121. http://dx.doi.org/10.1144/GSL.SP.2003.213.01.07.

Thordarson, T., Self, S., Óskarsson, N., Hulsebosch, T., 1996. Sulfur, chlorine, and fluorine degassing and atmospheric loading by the 1783 – 1784 AD Laki (Skaftár Fires) eruption in Iceland. Bull. Volcanol. 58, 205–225. http://dx.doi.org/10.1007/s004450050136.

Tolan, T.L., Reidel, S.P., Beeson, M.H., Anderson, J.L., Fecht, K.R., Swanson, D.A., 1989. of the Columbia River Basalt Group. Geol. Soc. Am. Spec. Pap. 239, 1–20. http://dx.doi.org/10.1130/SPE239-p1.

Torsvik, T.H., Cocks, L.R.M., 2009. The Lower Palaeozoic palaeogeographical evolution of the northeastern and eastern peri-Gondwanan margin from Turkey to New Zealand. Geol. Soc. London, Spec. Publ. 325, 3–21. http://dx.doi.org/10.1144/SP325.2.

Traves, D.M., 1955. The Geology of the Ord-Victoria Region, Northern Australia. Bur. Miner. Resour. Geol. Geophys. Bull. 27.

Truby, J.M., Mueller, S.P., Llewellin, E.W., Mader, H.M., 2015. The rheology of three-phase suspensions at low bubble capillary number. Proc. R. Soc. A Math. Phys. Eng. Sci. 471, 20140557. http://dx.doi.org/10.1098/rspa.2014.0557.

Veevers, J.J., 2001. Atlas of billion-year old earth history of Australia and neighbours in Gondwanaland. GEMOC Press, Sydney, Australia.

Vye-Brown, C., Self, S., Barry, T.L., 2013. Architecture and emplacement of flood basalt flow fields: case studies from the Columbia River Basalt Group, NW USA. Bull. Volcanol. 75, 697. http://dx.doi.org/10.1007/s00445-013-0697-2.

Wadge, G., 1981. The variation of magma discharge during basaltic eruptions. J. Volcanol. Geotherm. Res. 11, 139–168. http://dx.doi.org/10.1016/0377-0273(81)90020-2.

Waichel, B.L., Lima, E.F., Lubachesky, R., Sommer, C. a., 2006. Pahoehoe flows from the central Paraná Continental Flood Basalts. Bull. Volcanol. 68, 599–610. http://dx.doi.org/10.1007/s00445-005-0034-5.

Walker, G.P.L., 1973. Lengths of Lava Flows. Philos. Trans. R. Soc. London 274, 107–118. http://dx.doi.org/10.1098/rsta.1973.0030.

Walker, G.P.L., 1971. Compound and simple lava flows and flood basalts. Bull. Volcanol. 35, 579–590. http://dx.doi.org/10.1007/BF02596829.

Woods, A.W., 1993. A model of the plumes above basaltic fissure eruptions. Geophys. Res. Lett. 20, 1115–1118. http://dx.doi.org/10.1029/93GL01215.